Równania oscylacji

Skale czasowe w gwieździe
[wyprowadzamy razem na tablicy]

Podsumowanie lekcji 1-3
(Typy pulsacji, Kappa-mechanizm,
Z-maksymum)

Oscylacje $\beta$Cep *vs* SPB *vs* $\delta$Sct

# Równania małych oscylacji (teoria liniowa)

## 2.1 Równania gazodynamiki

Definicje:
$\boldsymbol{x}_0$ -współrzędne Lagranżowskie – identyfikują element gazu (n.p. położenie w chwili $t = 0$, lub w modelu niezaburzonym)
$\boldsymbol{x}$ -współrzędne Eulerowskie – podają aktualne położenie elementu w przestrzeni
$\frac{d}{dt}$ – pochodna Lagranżowska (śledcza); ustalone $\boldsymbol{x}_0$
$\frac{\partial}{\partial t}$ – pochodna Eulerowska; ustalone $\boldsymbol{x}$

$$\frac{d}{dt} = \frac{\partial}{\partial t} + \boldsymbol{v} \cdot \boldsymbol{\nabla}, \tag{2.1}$$

gdzie $\boldsymbol{v} = \frac{d\boldsymbol{x}}{dt}$ – prędkość elementu.
Równanie ruchu:

$$\rho \frac{d\boldsymbol{v}}{dt} = -\boldsymbol{\nabla} P - \rho \boldsymbol{\nabla} \Phi. \tag{2.2}$$

Równanie ciągłości:

$$\frac{\partial \rho}{\partial t} = -\boldsymbol{\nabla} \cdot (\rho \boldsymbol{v}). \tag{2.3}$$

Równanie Poissona:

$$\boldsymbol{\nabla}^2 \Phi = 4\pi G \rho. \tag{2.4}$$

**W.A.Dziembowski, wyklad „Astroseismologia”, file mon02.pdf.**

## 2.1 Równania gazodynamiki

Definicje:
$\boldsymbol{x}_0$ -współrzędne Lagranżowskie – identyfikują element gazu (n.p. położenie w chwili $t = 0$, lub w modelu niezaburzonym)
$\boldsymbol{x}$ -współrzędne Eulerowskie – podają aktualne położenie elementu w przestrzeni
$\frac{d}{dt}$ – pochodna Lagranżowska (śledcza); ustalone $\boldsymbol{x}_0$
$\frac{\partial}{\partial t}$ – pochodna Eulerowska; ustalone $\boldsymbol{x}$

$$\frac{d}{dt} = \frac{\partial}{\partial t} + \boldsymbol{v} \cdot \boldsymbol{\nabla}, \tag{2.1}$$

gdzie $\boldsymbol{v} = \frac{d\boldsymbol{x}}{dt}$ – prędkość elementu.
Równanie ruchu:

$$\rho \frac{d\boldsymbol{v}}{dt} = -\boldsymbol{\nabla} P - \rho \boldsymbol{\nabla} \Phi. \tag{2.2}$$

Równanie ciągłości:

$$\frac{\partial \rho}{\partial t} = -\boldsymbol{\nabla} \cdot (\rho \boldsymbol{v}). \tag{2.3}$$

Równanie Poissona:

$$\boldsymbol{\nabla}^2 \Phi = 4\pi G \rho. \tag{2.4}$$

Warunek adiabatyczności:

$$\frac{dP}{dt} = c^2 \frac{d\rho}{dt}, \tag{2.5}$$

gdzie $c^2 = \Gamma_1 \frac{P}{\rho}$ prędkość dźwięku.

**W.A.Dziembowski, wyklad „Astroseismologia”, file mon02.pdf.**

**Dla uwzględnienia nieadiabatyczności**
**dodajemy równanie zachowania energii oraz równanie transferu promienistego:**

We need to consider the heat gain in more detail. Specifically, it can be written as

$$\rho \frac{\mathrm{d}q}{\mathrm{d}t} = \rho\,\epsilon - \mathrm{div}\,\mathbf{F}\ ; \tag{3.21}$$

here $\epsilon$ is the rate of energy generation per unit mass (*e.g.* from nuclear reactions), and $\mathbf{F}$ is the flux of energy. In general, radiation is the only significant contributor to the energy flux; in particular, molecular conduction is almost always negligible.

The general calculation of the radiative flux is also non-trivial. In stellar atmospheres the full radiative transfer problem, as known from the theory of the structure of stellar atmospheres, must be solved in combination with the hydrodynamic equations. This is another active area of research, and the subject of a major monograph (Mihalas & Mihalas 1984). In stellar interiors the diffusion approximation is adequate, and the radiative flux is given by

$$\mathbf{F} = -\frac{4\pi}{3\kappa\rho}\,\nabla B = -\frac{4a\tilde{c}T^3}{3\kappa\rho}\,\nabla T\ , \tag{3.22}$$

**JCD 1997, Lecture Notes on Stellar Oscillations, Chapter 3.**

# Równania małych oscylacji

## Pochodne (zaburzenia ) Eulerowskie i Lagranżowskie , linearyzacja

$$\frac{d}{dt} = \frac{\partial}{\partial t} + \boldsymbol{v} \cdot \boldsymbol{\nabla}$$

$$\boldsymbol{v} = \frac{d\boldsymbol{x}}{dt}$$

$$\boldsymbol{\xi} = \boldsymbol{x} - \boldsymbol{x}_0$$

$$\boldsymbol{v} = \frac{d\boldsymbol{\xi}}{dt} = \frac{\partial \boldsymbol{\xi}}{\partial t}$$

$$\delta\rho = \rho' + \boldsymbol{\xi} \cdot \boldsymbol{\nabla}\rho = \rho' + \xi_r (\frac{d\rho}{dr})_0$$

# Równania małych oscylacji adiabatycznych

**równanie ciągłości:** $\frac{\partial \rho}{\partial t} = -\nabla \cdot (\rho \boldsymbol{v})$ $\longrightarrow$ $\rho' = -\nabla \cdot (\rho \boldsymbol{\xi})$

**adiabatyczność:** $\frac{dP}{dt} = c^2 \frac{d\rho}{dt}$ $\longrightarrow$ $P' = \rho(g\boldsymbol{\xi}_r - c^2 \nabla \cdot \boldsymbol{\xi})$

**równanie Poissona:** $\nabla^2 \Phi = 4\pi G \rho$ $\longrightarrow$ $\Phi' = G \int \frac{\nabla_d \cdot (\rho \boldsymbol{\xi}) d^3 \boldsymbol{x}_d}{|\boldsymbol{x} - \boldsymbol{x}_d|}$

**równanie ruchu** $\rho \frac{d\boldsymbol{v}}{dt} = -\nabla P - \rho \nabla \Phi$ $\longrightarrow$ $\omega^2 \rho \boldsymbol{\xi} = \boldsymbol{L}(\boldsymbol{\xi})$

$$\boldsymbol{L}(\boldsymbol{\xi}) = \nabla[\rho(g\boldsymbol{\xi}_r - c^2 \nabla \cdot \boldsymbol{\xi})] - g\boldsymbol{e}_r \nabla \cdot (\rho \boldsymbol{\xi}) + \rho \nabla \left( G \int \frac{\nabla_d \cdot (\rho \boldsymbol{\xi}) d^3 \boldsymbol{x}_d}{|\boldsymbol{x} - \boldsymbol{x}_d|} \right)$$

**W.A.Dziembowski, wyklad „Astroseismologia”, file m02.ppt**

# Równania na funkcje własne (oscylacje adiabatyczne)

$$\boldsymbol{\xi} = r[y_1(r)\boldsymbol{e}_r + z(r)\boldsymbol{\nabla}_H]Y_\ell^m exp(-i\omega t)$$

$$\Phi' + \frac{P'}{\rho} = g r y_2 Y_\ell^m \exp(-i\omega t)$$

$$\Phi' = g r y_3 Y_\ell^m \exp(-i\omega t)$$

$$\frac{d\Phi'}{dr} = g y_4 Y_\ell^m \exp(-i\omega t)$$

$$\frac{dy_1}{d\ln r} = (V_g - 3)y_1 + [\frac{\ell(\ell+1)}{C\sigma^2} - V_g]y_2 + V_g y_3$$

$$\frac{dy_2}{d\ln r} = (C\sigma^2 - A + U\delta_{l,0})y_1 + (1 + A - U)y_2 - Ay_3$$

$$\frac{dy_3}{d\ln r} = (1 - U)y_3 + y_4$$

$$\frac{dy_4}{d\ln r} = UAy_1 + UV_g y_2 + [\ell(\ell+1) - UV_g]y_3 - Uy_4$$

$\ell = 0$

$y_3 \equiv 0 \quad y_4 = -Uy_1$

$\sigma^2$ **wartość własna**

$V_g \quad C \quad A \quad U$

**z modelu gwiazdy**

## Równania nieadiabatycznych oscylacji.

Following the standard procedure, we assume spherical harmonic, $Y_{l,j}(\vartheta, \varphi)$, angular dependence and exponential, $\exp(\omega t)$, time dependence for the first order quantities. Thus, the oscillation period given by $P = 2\pi/\omega_I$, where $\omega_I = \mathrm{Im}(\omega)$, and $\omega_R = \mathrm{Re}(\omega)$, if positive, gives the excitation rate.

In this way, the equations are reduced to a sixth-order, complex eigenvalue problem with $\omega$ being the eigenvalue, for each $l$ (it is well-known that $j$ does not enter the equations). Here we shall write the equations in the form of six first-order equations for the following $r$-dependent variables:

$$d = [\xi_r/r], \qquad p = [\Delta P/P], \qquad w = [\delta W r/GM_r],$$

$$w_1 = \left[\frac{r^2}{GM_r}\frac{d\delta W}{dr}\right], \qquad s = \left[\frac{\Delta T}{T} - \nabla_{ad}\frac{\Delta P}{P}\right], \qquad f = \left[\Delta(4\pi r^2 F_r)\right]\frac{1}{L},$$

where symbol [ ] means that we take only the $r$-dependent part of the variable; $\xi_r$ is the radial component of the displacement; $F_r$ is local radiative flux, $L$ is surface luminosity and $W$ is gravitational potential. $\Delta$ and $\delta$ denote the Lagrangian and Eulerian perturbations, respectively. The remaining symbols have their usual meaning.

**W.A.Dziembowski, 1977, Acta Astr., 27, 95.**

We moreover introduce a nondimensional frequency $\sigma = \omega/\sqrt{4\pi G\langle\varrho\rangle}$. Choosing $\ln x = \ln(r/R) = A_1$ for the independent variable and denoting the differentation by $'$ we may write our basic equations as follows

$$d' = -d(3+\eta) - p(\eta_1 + A_4) - w\eta - sA_7, \tag{1}$$

$$p' = A_3[d(4 - A_2\sigma^2 - A_5 + \eta) + p(1+\eta_1) + w\eta - w_1], \tag{2}$$

$$w' = w(1 - A_5) + w_1, \tag{3}$$

$$w_1' = A_5[d(A_6 + A_3A_4) + pA_4 - w_1 + sA_7] + wl(l+1), \tag{4}$$

$$s' = A_3A_8\{d[A_{10}(A_2\sigma^2 + A_5) + (4+\eta)(1-A_{10})] + p[\eta_1(1-A_{10}) - A_9] + w\eta(1-A_{10}) + w_1A_{10} - sA_{11} - fA_{12}\}, \tag{5}$$

$$f' = -d[\eta E + l(l+1)/A_{12}] + p[(\varepsilon_p - \eta_1)E - l(l+1)/A_3A_{12}], \tag{6}$$

$$-w\eta E - s[A_{13}\sigma - \varepsilon_s E + l(l+1)/A_3A_8A_{12}],$$

W.A.Dziembowski, 1977, Acta Astr., 27, 95.

where

$$A_2 = \frac{4\pi r^3 \langle \varrho \rangle}{M_r}, \qquad A_3 = -\left(\frac{\mathrm{d}\ln P}{\mathrm{d}\ln r}\right)_0,$$

$$A_4 = \frac{1}{\Gamma_1}, \qquad A_5 = \frac{4\pi r^3 \varrho}{M_r},$$

$$A_6 = \frac{1}{\Gamma_1}\left(\frac{\mathrm{d}\ln P}{\mathrm{d}\ln r}\right)_0 - \left(\frac{\mathrm{d}\ln \varrho}{\mathrm{d}\ln r}\right)_0, \qquad A_7 = \left(\frac{\partial \ln \varrho}{\partial \ln P}\right)_T,$$

$$A_8 = \nabla = \left(\frac{\mathrm{d}\ln T}{\mathrm{d}\ln P}\right)_0, \qquad A_9 = \left[\frac{\partial \ln(\varkappa/T^4)}{\partial \ln P}\right]_{ad} + A_{10} - \left(\frac{\mathrm{d}\nabla_{ad}}{\mathrm{d}\ln T}\right)_0,$$

$$A_{10} = \frac{\nabla_{ad}}{\nabla}, \qquad A_{11} = \left[\frac{\partial \ln(\varkappa T^4)}{\partial s}\right]_p$$

$$A_{12} = \frac{L}{L_r}, \qquad A_{13} = \frac{\sqrt{4\pi G \langle \varrho \rangle}}{L}\,\frac{4\pi r^3 P(-A_7)}{\nabla_{ad}}$$

W.A.Dziembowski, 1977, Acta Astr., 27, 95.

$$\eta = \frac{l(l+1)}{A_2 \sigma^2}, \qquad \eta_1 = \frac{\eta}{A_3}$$

$$E = \frac{4\pi r^3 \varrho \varepsilon}{L_r} = -\left(\frac{\mathrm{d}\ln A_{12}}{\mathrm{d}\ln_r}\right)_0,$$

$$\varepsilon_p = \left(\frac{\partial \ln \varepsilon}{\partial \ln P}\right)_{ad}, \qquad \varepsilon_s = \left(\frac{\partial \ln \varepsilon}{\partial s}\right)_p.$$

The unexplained symbols have their usual meaning. Thus, the elements of matrix $A$ transmit all the information about stellar model that is needed for oscillation calculation; the derivatives of $\varepsilon$, being unimportant in the present study, were ignored.

We do not give the details of the derivation of equations, because it is easy to obtain Eq. (1) from the continuity equation and the horizontal component of the momentum equation; Eq. (2) from the radial component of the momentum equation; Eqs. (3) and (4) from the Poisson equation, Eq. (5) from the radial component of the radiative transport equation combined with Eq. (2); and Eq. (6) from the energy equation.

**W.A.Dziembowski, 1977, Acta Astr., 27, 95.**

Three outer boundary conditions for our equations are applicable in the stellar atmosphere at low optical depth. Two condition are the same as in the adiabatic case (see *e.g.* Dziembowski 1971), namely

$$p'/A_3 = 0, \qquad w_1 + (l+1)w = 0. \tag{7}$$

The first of these results from the assumption of the total wave reflection in the isothermal atmosphere. The second follows from fitting the gravitational potential perturbation to the decreasing solution of the Laplace equation, which is justified because the distortion of the outermost stellar layers produces negligible gravitational effect.

The third condition is given by linearization of the blackbody condition:

$$4(s + p\nabla_{ad}) + 2d - f = 0, \tag{8}$$

The inner boundary conditions may be found analysing the singularity at $x \to 0$. However, since equations (1)-(6) are never integrated up to the center, we shall not write them explicitly. The actual form the inner boundary conditions will be given in sections 4 and 5.

There are several important cases in which the original 6-th order equation system may be reduced to some lower-order system.

**W.A.Dziembowski, 1977, Acta Astr., 27, 95.**

# Skale czasowe w gwieździe [wyprowadzamy razem na tablicy]

**Charakterystyczne scale czasowe wewnątrz gwiazdy**

~ J. Chr.-Dals., A. Maeder et al

## Characteristic stellar timescales

- **The dynamical timescale**

The free-fall time for distance $\ell$ in the grav. field of star:

$$t = \sqrt{\frac{2\ell}{g}} = \sqrt{\frac{2\ell R^2}{GM}}$$

$$\ell \sim R \Rightarrow t_{dyn} \sim \sqrt{\frac{2R^3}{GM}}$$

$G = 6.7_{10}-8$, $R_\odot \simeq 7_{10}10$, $M_\odot \simeq 2_{10}33$

$t_{dyn}^\odot \sim 40$ minutes

$$t_{dyn} \sim 40 \cdot \sqrt{\frac{(R/R_\odot)^3}{M/M_\odot}} \text{ minutes}$$

- **The thermal timescale** (the timescale for release of gravitational energy at a rate $L$)

Work to bring $\delta M_r$ from $\infty$ to radius $r$:

$$\delta W = GM_r \delta M_r \int_{-\infty}^{r} \frac{dr}{r^2} = -\frac{GM_r}{r}\delta M_r$$

$$\delta\Omega = \delta W, \quad \Omega = -G\int_0^M \frac{M_r dM_r}{r} \simeq -q\frac{GM^2}{R}$$

$q \sim \frac{3}{2}$ for MS

$$t_{th} = q\frac{GM^2}{RL}$$

$t_{th}^\odot \simeq 47_{10}6$ yrs

$$t_{th} = 47_{10}6 \frac{(M/M_\odot)^2}{(R/R_\odot)\cdot(L/L_\odot)}$$

- **The nuclear timescale**

$$\Delta E = \Delta m \cdot c^2, \quad \frac{4m_H}{m_{He}} = \frac{4 \cdot 1.008}{4.0026} \simeq 1.007$$

Nuclear reactions - in inner ~10% of mass

$$t_{nuc} \sim \frac{1}{10}\cdot\frac{0.007Mc^2}{L} \qquad t_{nuc}^\odot \simeq 10^{10} \text{ yrs}$$

$$t_{nuc} = \frac{M/M_\odot}{L/L_\odot}\cdot 10^{10} \text{ yrs}$$

Stars whose luminosity varies periodically have been known for centuries. However, only within the last hundred years has it been definitely established that in many cases these variations are due to *intrinsic* pulsations of the stars themselves. For obvious reasons studies of pulsating stars initially concentrated on stars with large amplitudes, such as the Cepheids and the long period variables. The variations of these stars could be understood in terms of pulsations in the fundamental radial mode, where the star expands and contracts, while preserving spherical symmetry. It was realized very early (Shapley 1914) that the period of such motion is approximately given by the dynamical time scale of the star:

$$t_{\rm dyn} \simeq \left(\frac{R^3}{GM}\right)^{1/2} \simeq (G\bar{\rho})^{-1/2} \,, \tag{1.1}$$

where $R$ is the radius of the star, $M$ is its mass, $\bar{\rho}$ is its mean density, and $G$ is the gravitational constant. Thus observation of the period immediately gives an estimate of one intrinsic property of the star, *viz.* its mean density.

It is a characteristic property of the Cepheids that they lie in a narrow, almost vertical strip in the HR diagram, the so-called *instability strip*. As a result, there is a direct relation between the luminosities of these stars and their radii; assuming also a mass-luminosity relation one obtains a relation between the luminosities and the periods, provided that the latter scale as $t_{\rm dyn}$. This argument motivates the existence of a *period-luminosity relation* for the Cepheids: thus the periods, which are easy to determine observationally, may be used to infer the intrinsic luminosities; since the apparent luminosities can be measured, one can determine the distance to the stars. This provides one of the most important distance indicators in astrophysics.

The main emphasis in the early studies was on understanding the causes of the pulsations, particularly the concentration of pulsating stars in the instability strip. As in many other branches of astrophysics major contributions to the understanding of stellar pulsation were made by Eddington (*e.g.* Eddington 1926). However, the identification of the actual cause of the pulsations, and of the reason for the instability strip, was first arrived at independently by Zhevakin (1953) and by Cox & Whitney (1958).

# Typy pulsacji gwiazd

**Według geometrii pulsacji:**

**Radialne - drgania z zachowaniem symetrii sferycznej, węzły dla obertonów - tylko wzdłuż promienia, jako koncentryczne sfery.**
**Nieradialne – na sferze mamy obszary, które drgają w przeciwfazie.**

**Według fizycznej natury:**

**Akustyczne (ciśnieniowe) [np. fale dźwiękowe] , dla których siłą zwracającą jest gradient ciśnienia. Radialne pulsacje należą do akustycznych.**
**Grawitacyjne [np. fale na wodzie], dla których siłą zwracającą jest grawitacja. Tylko nieradialne pulsacje.**

# MODY

$$\frac{\delta T}{T} = y_{T,n}(r) Y_\ell^m(\theta,\phi) \exp(-\mathrm{i}\omega_{n\ell m} t)$$

$y_{T,n}(r)$ radialna funkcja własna

$Y_\ell^m(\theta,\phi)$ sferyczna harmonika

$n$ radialny rząd modu

$\nabla_H^2 Y = -\ell(\ell+1)Y$

$\ell$ stopień modu

$n < 0$ mody **g** $(\ell > 0)$

$n = 0$ mody **f** $(\ell > 1)$

$n > 0$ mody **p**

$m = -\ell, \ldots 0, \ldots \ell$ rząd azymutalny

$$Y_\ell^m(\theta,\phi) = (-1)^m \mathcal{N}_\ell^{|m|} P_\ell^{|m|}(\mu) \exp(\mathrm{i}m\phi)$$

$$\mathcal{N}_\ell^{|m|} = \sqrt{\frac{(2\ell+1)(\ell-|m|)!}{4\pi(\ell+|m|)!}}$$

$\mu = \cos\theta$

$$P_\ell^{|m|}(\mu) = (1-\mu^2)^{\frac{|m|}{2}} \frac{d^{|m|} P_\ell}{d\mu^{|m|}}$$

- stowarzyszone funkcje Legendra

$P_\ell$ - wielomiany Legendra

**W. A. Dziembowski**

# MODY

$$\frac{\delta T}{T} = y_{T,n}(r) Y_\ell^m(\theta,\phi) \exp(-\mathrm{i}\omega_{n\ell m} t)$$

$y_{T,n}(r)$ radialna funkcja własna

$Y_\ell^m(\theta,\phi)$ sferyczna harmonika

$n$ radialny rząd modu

$\nabla_H^2 Y = -\ell(\ell+1)Y$

$n<0$ mody **g** $(\ell > 0)$

$\ell$ stopień modu

$n=0$ mody **f** $(\ell > 1)$

$m = -\ell, \ldots 0, \ldots \ell$ rząd azymutalny

$n>0$ mody **p**

częstotliwość kołowa $\omega_{n,\ell,m} = 2\pi\nu_{n,\ell,m}$

najniższy mod radialny $\omega_{1,0,0} = \sigma_{1,0,0}\sqrt{4\pi G\bar{\rho}}$ $\sigma_{1,0,0} \in (1.4, 2)$

mody wyższe (owertony) $\omega_{n+1,0,0} > \omega_{n,0,0}$

mody nieradialne $\omega_{n+1,\ell,m} > \omega_{n\ell,m}$

gwiazdy sferyczne $\omega_{n,\ell,m} = \omega_{n,\ell,0}$

**W. A. Dziembowski**

# Przykłady geometrii oscylacji nieradialnych:

a) $l$=1, m=0
b) $l$=1, m=1

c) $l$=2, m=0
d) $l$=2, m=1
e) $l$=2, m=2

f) $l$=3, m=0
g) $l$=3, m=1
h) $l$=3, m=2
i) $l$=3, m=3

j) $l$=5, m=5
k) $l$=10, m=5
l) $l$=10, m=10

J. Christensen-Dalsgaard

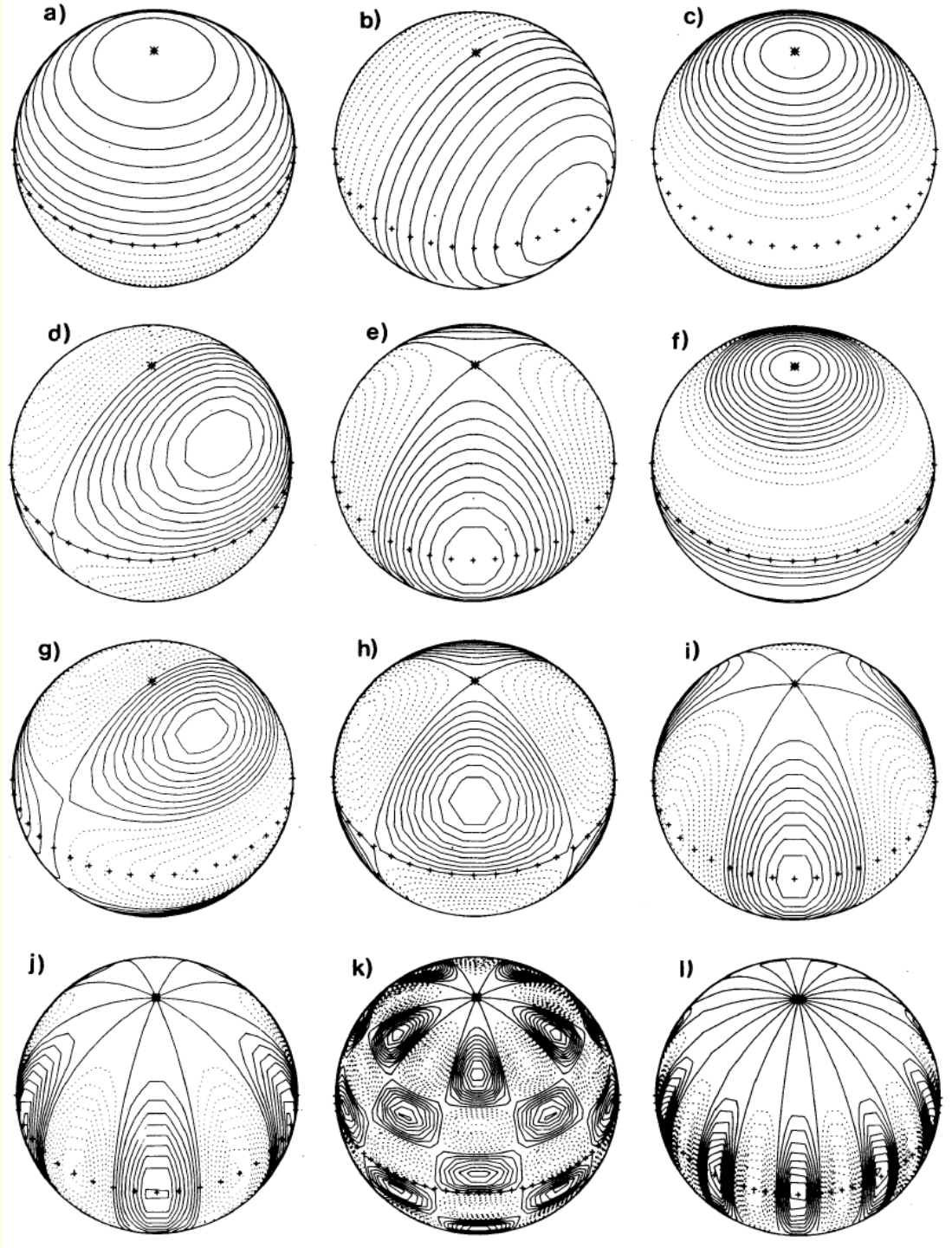

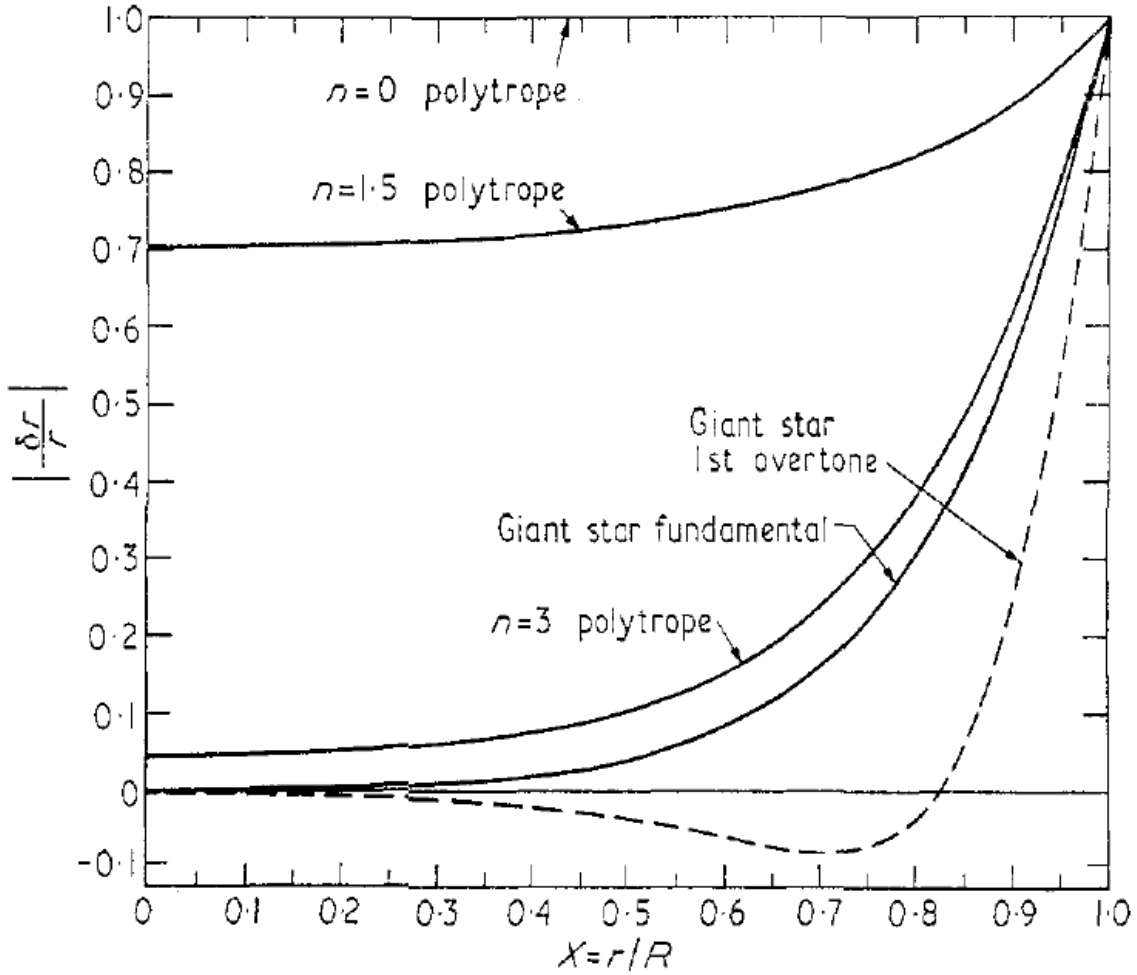


**Figure 14.** Eigenfunctions for the fundamental (solid lines) and first harmonic (broken line) modes for selected stellar models. Abscissa is fractional distance from the stellar centre; ordinate is relative radius semi-amplitude.

Cox 1974

Frequencies of non radial modes of the homogeneous model

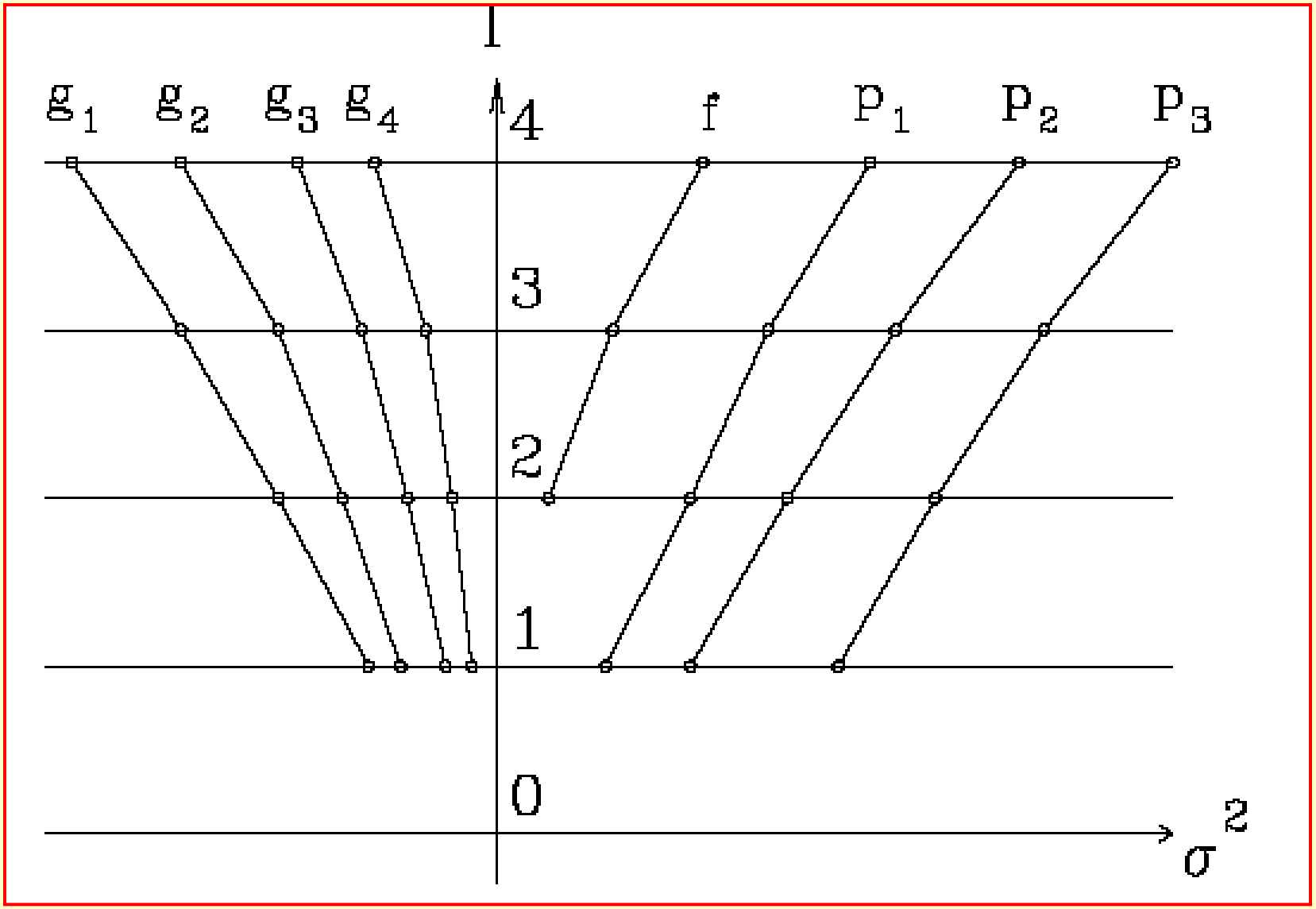


R. Scuflaire

***Lokalne własności oscylacji są opisane przez dwie charakterystyczne częstotliwości:***

1. ***częstotliwość Lamba, $L_\ell^2$***
2. ***częstotliwość Brunta-Väisälä, $N^2$***

$$L_\ell^2=(k_h c)^2= \ell(\ell+1)\, c^2/r^2$$

$$k_h = 2\pi/\lambda_h\,, \quad c^2=\Gamma_1 p/\rho\,, \quad \Gamma_1=(d\ln p/d\ln\rho)_{ad}$$

***$k_h$ - falowa liczba horyzontalna, $\Gamma_1$ - wykładnik adiabaty***
***$\lambda_h$ – horyzontalna długość fali***

$$k_h= [\ell(\ell+1)]^{1/2}/r \approx \ell/r$$

***Fala akustyczna pokonuje drogę $\lambda_h = 2\pi r/\ell$ ruchem horyzontalnym z okresem $2\pi/L$, gdzie $L= [\ell(\ell+1)]^{1/2}$.***

**Z wykładu J. Daszyńskiej-Daszkiewicz**

## *Częstotliwość Brunta-Väisälä, $N^2$*

$$N^2 = g\left(\frac{1}{\Gamma_1}\frac{d\ln p}{dr} - \frac{d\ln \rho}{dr}\right)$$

***$N^2$ – częstotliwość z jaką element gazu może oscylować wokół położenia równowagi po wpływem siły grawitacji***

**Z wykładu J. Daszyńskiej-Daszkiewicz**

$\omega^2 > L_\ell^2, N^2$

***mody o wysokich częstotliwościach (ciśnieniowe)***

$\omega^2 < L_\ell^2, N^2$

***mody o niskich częstotliwościach (grawitacyjne)***

$L_\ell^2 > \omega^2 > N^2$ ***lub*** $L_\ell^2 < \omega^2 < N^2$

***obszary znoszenia oscylacji***

**Z wykładu J. Daszyńskiej-Daszkiewicz**

# Propagation diagram, ZAMS solar model

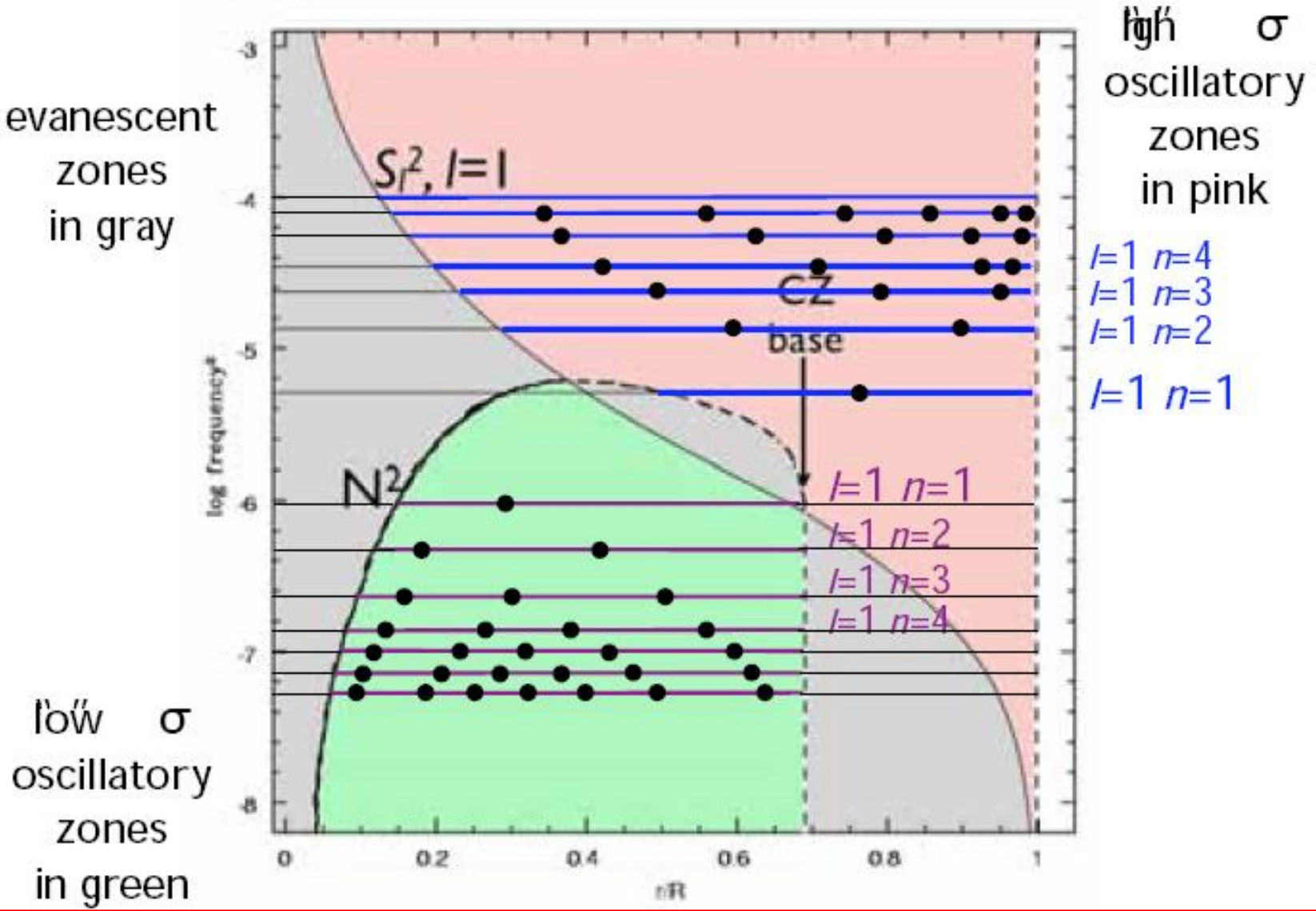


(Kawaler, Lecture 3)

# Diagramy propagacji akustycznych i grawitacyjnysh oscylacji

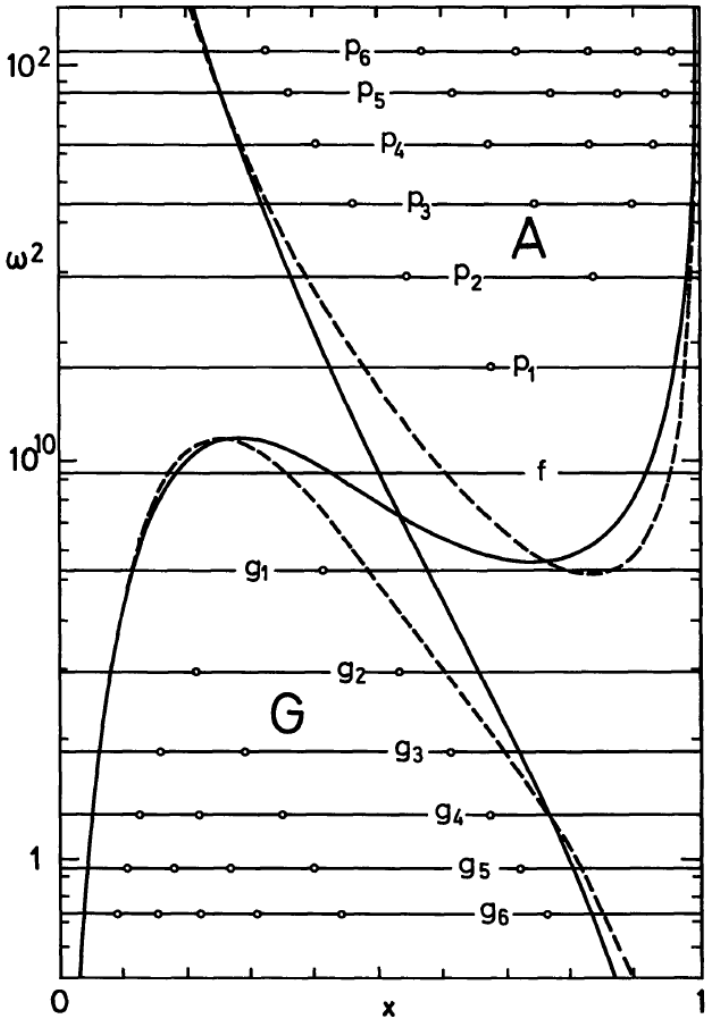


Fig. 4. Polytrope of index 3. The solid lines delimit $A$ and $G$ regions. The horizontal lines give the frequencies of a few modes ($l=2$) and the circles represent the positions of their nodes. The dashed lines represent the cut-off frequencies for plane waves

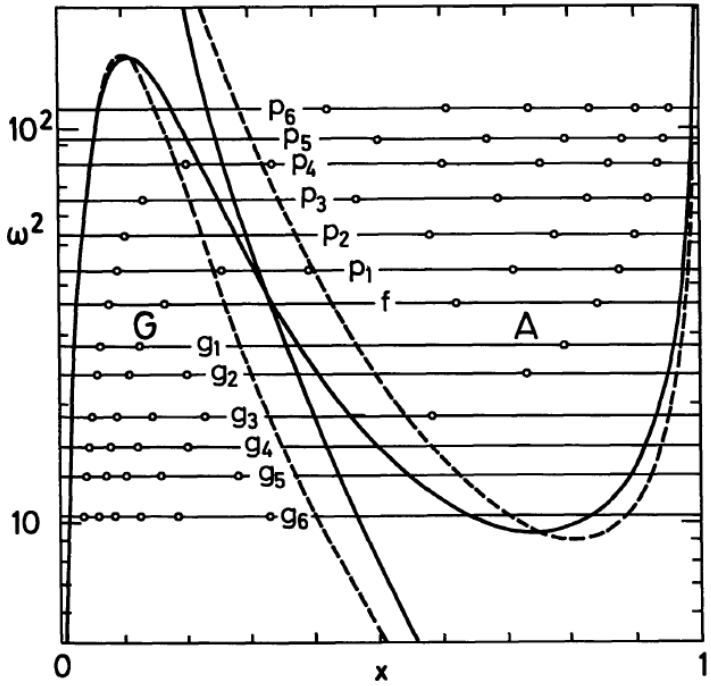


Fig. 5. Same as Fig. 4 but for the polytrope of index 4

the $A$ region and all the nodes of the $g$ modes lie in the $G$ region as it is expected. But for the more condensed polytrope $n=4$ ($\varrho_c/\overline{\varrho}=622.4$, Fig. 5) the $f$ mode and the first $p$ and $g$ modes have nodes in both regions. We can no longer say that these $p$ modes are purely acoustic modes. They have rather a mixed character: gravity waves in the internal regions and acoustic waves in the external layers. The same is true for the first $g$ modes. This transition from a gravity wave to

**Scuflaire 1974**

## Mody grawitacyjne

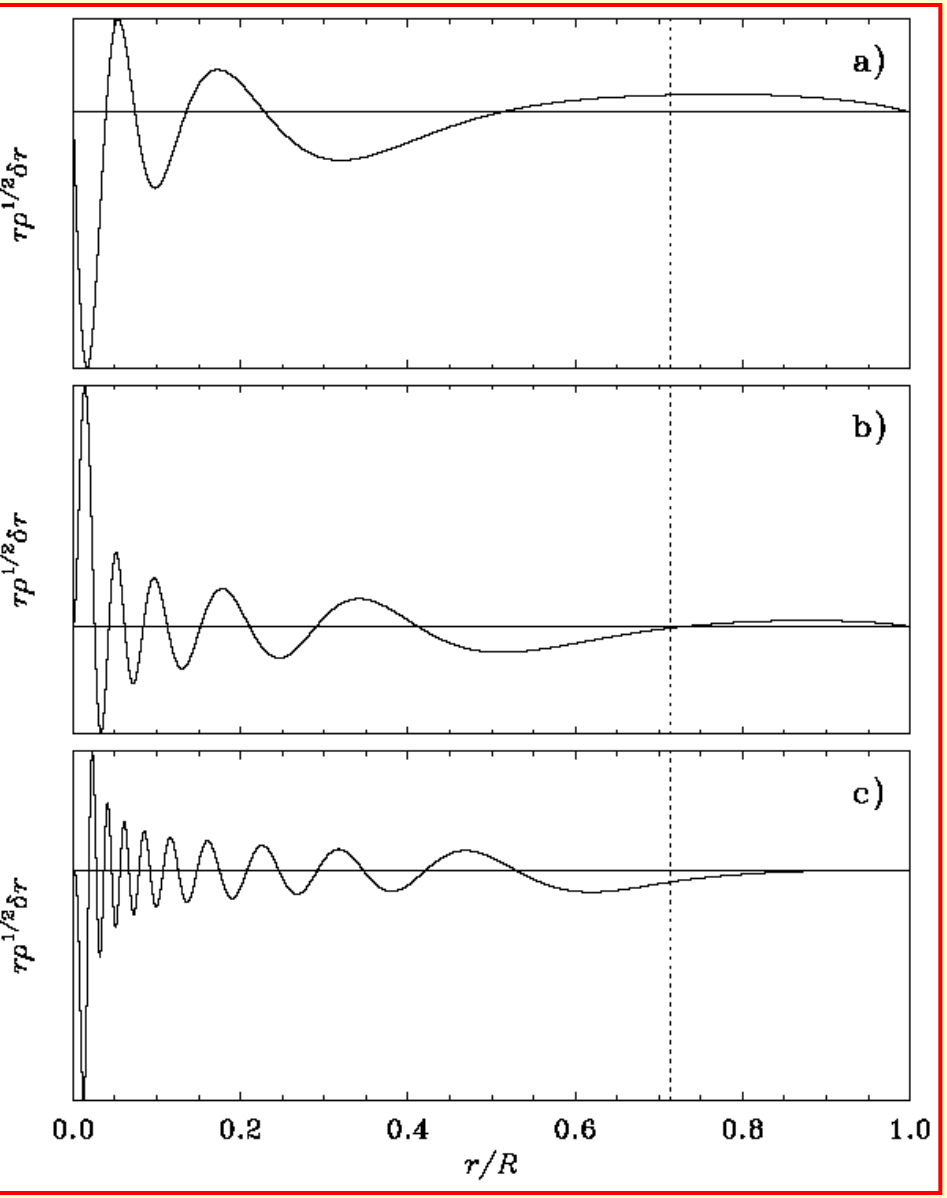


(l,n)=(1,5), (2,10), (4,19), ν=100μHz

## Mody akustyczne (ciśnieniowe)

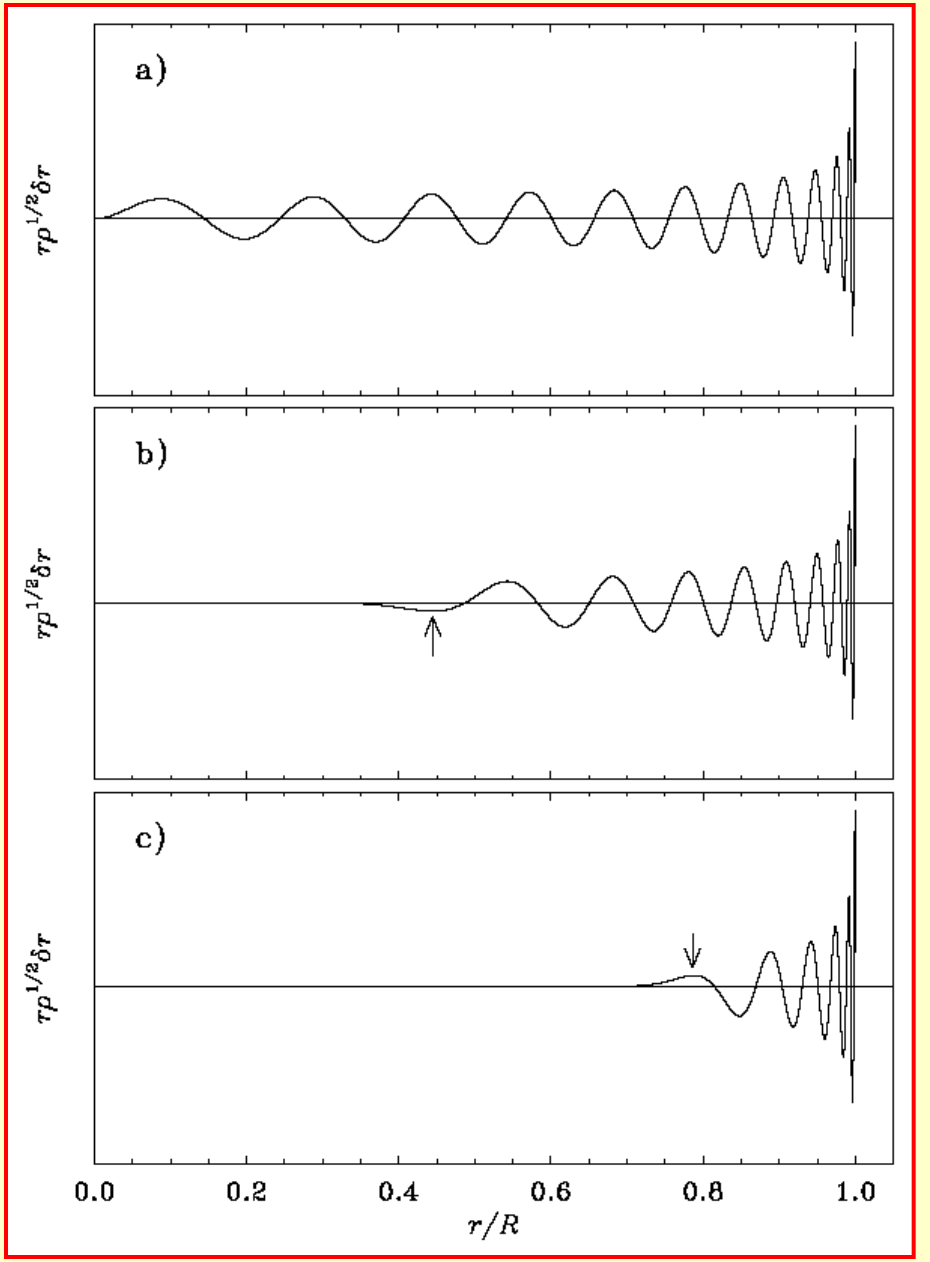


(l,n)=(0,23), (20,17), (60,10), ν=3300μHz

**Oscillation frequencies of typical Beta Cephei and Delta Scuti models on the main sequence**

**(from the ZAMS to the TAMS)**

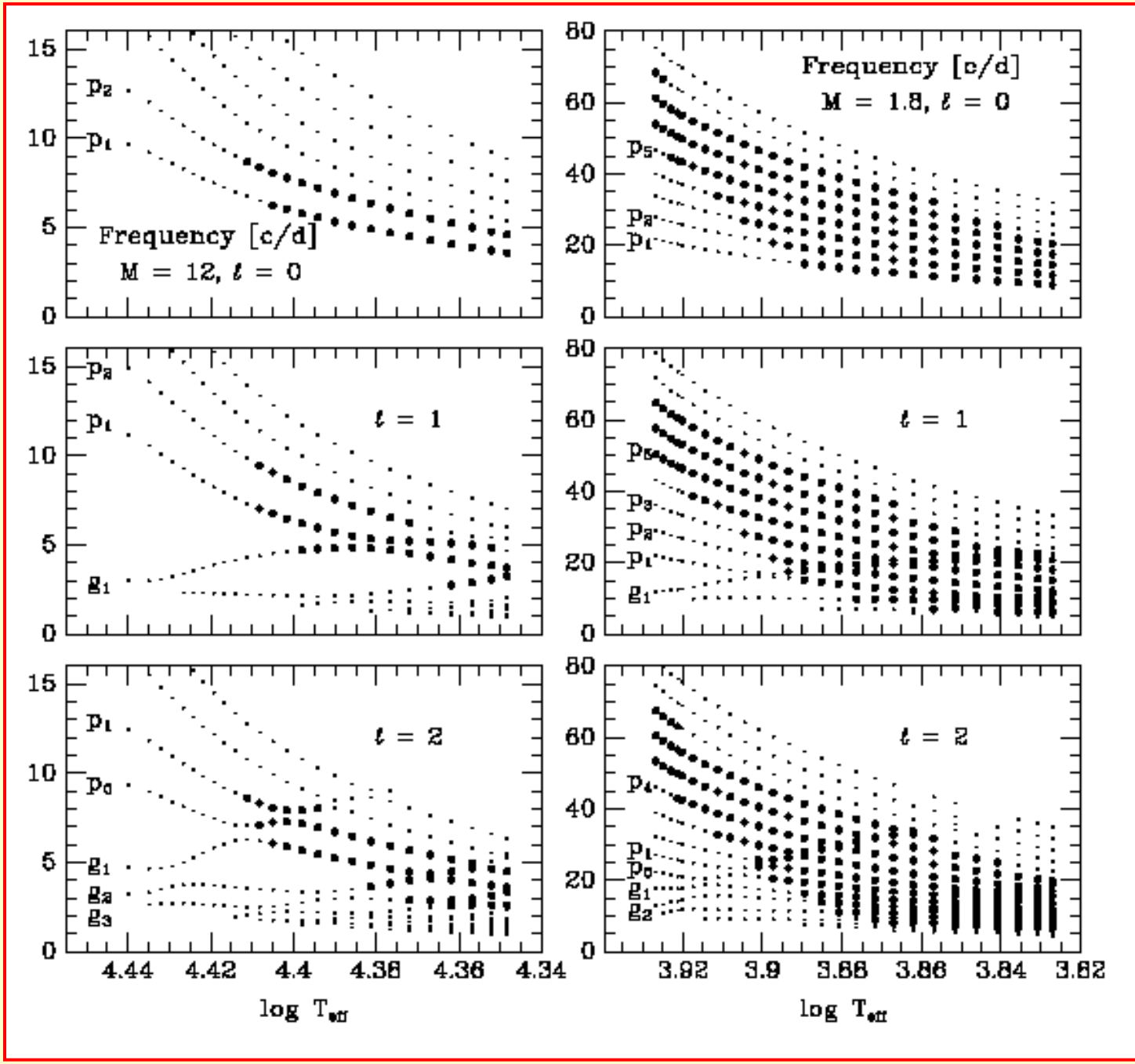

## Regularities in theoretical frequency spectra:

- high-order p-modes:

$$\nu_{nl} \approx \Delta\nu \cdot \left(n + \frac{l}{2} + \alpha\right) - \frac{l(l+1)}{4\pi^2 n} \cdot f_c$$

$$\Delta\nu = \left(2\int \frac{dr}{c}\right)^{-1}, \quad f_c = \int \frac{dc}{dr} \cdot \frac{dr}{r}$$

large separation:

$$\nu_{nl} - \nu_{n-1,l} \approx \Delta\nu$$

small separation:

$$\nu_{nl} - \nu_{n-1,l+2} = \delta\nu_{nl} \approx -\frac{4l+6}{4\pi^2 n} \cdot f_c$$

- high-order g-modes:

$$\Pi_{nl} \approx \frac{n}{\sqrt{l(l+1)}} \cdot \Delta\Pi, \quad \Delta\Pi = 2\pi^2 \left(\int \frac{N}{r}\, dr\right)^{-1}$$

$$N = g\left(\frac{1}{\Gamma_1}\frac{d\ln P}{dr} - \frac{d\ln \rho}{dr}\right)$$

- Rotational splitting: (~ Goupil et al. 2000)

$$\nu_m = \nu_0 + m\left(1 - C_{nl}\right)\frac{\Omega}{2\pi} + \frac{\Omega^2}{2\pi\nu_0}\left(D_0 + m^2 D_1\right) + m\frac{\Omega^3}{\nu_0^2}T$$

$$\Rightarrow \frac{\nu_m - \nu_{m=0}}{m} = \frac{\Omega}{2\pi}\left(1 - C_{nl} + m\mu D_1 + \mu^2 T\right)$$

$$\mu = \frac{\Omega}{\nu_0}$$

- rotation rate:

$$\frac{\nu_m - \nu_{-m}}{2m} = \Omega\left(1 - C_{nl} + \mu^2 T\right)$$

# Wzbudzanie pulsacji w klasycznym pasie niestabilności i na Ciągu Głównym: mechanizm „kappa” i Z-maksimum

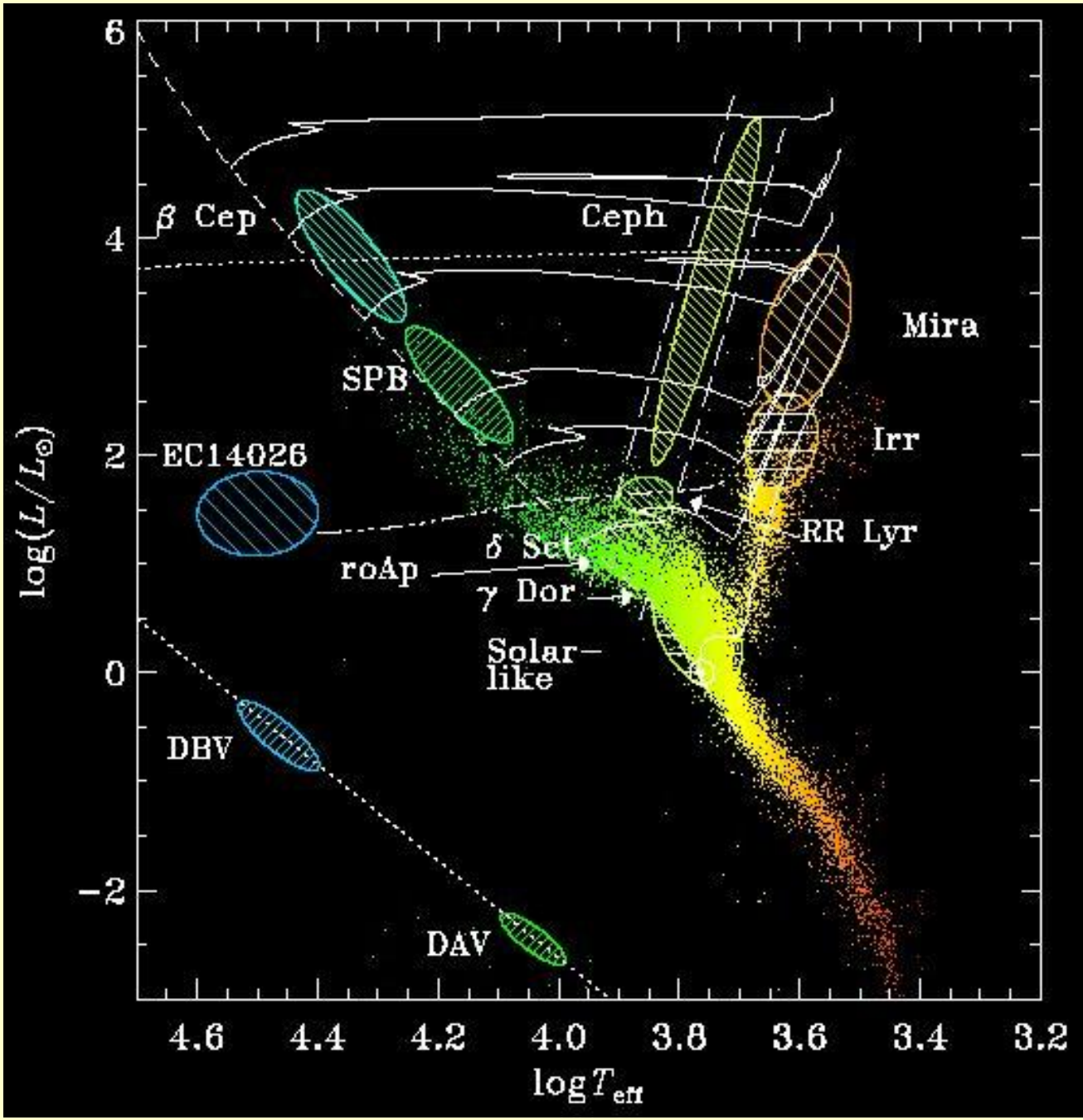


J. Christensen-Dalsgaard

# Całka pracy (Work integral)

Explicitly, we have

$$W = \int_M \mathrm{d}m \oint P\,\mathrm{d}V = \int_M \mathrm{d}m \int_0^{\Pi} P \frac{\partial}{\partial t}\left(\frac{1}{\rho}\right) \mathrm{d}\cancel{m}\,\mathrm{dt} \qquad (5.63)$$

and growth or decay correspond, respectively, to $W > 0$ or $W < 0$.

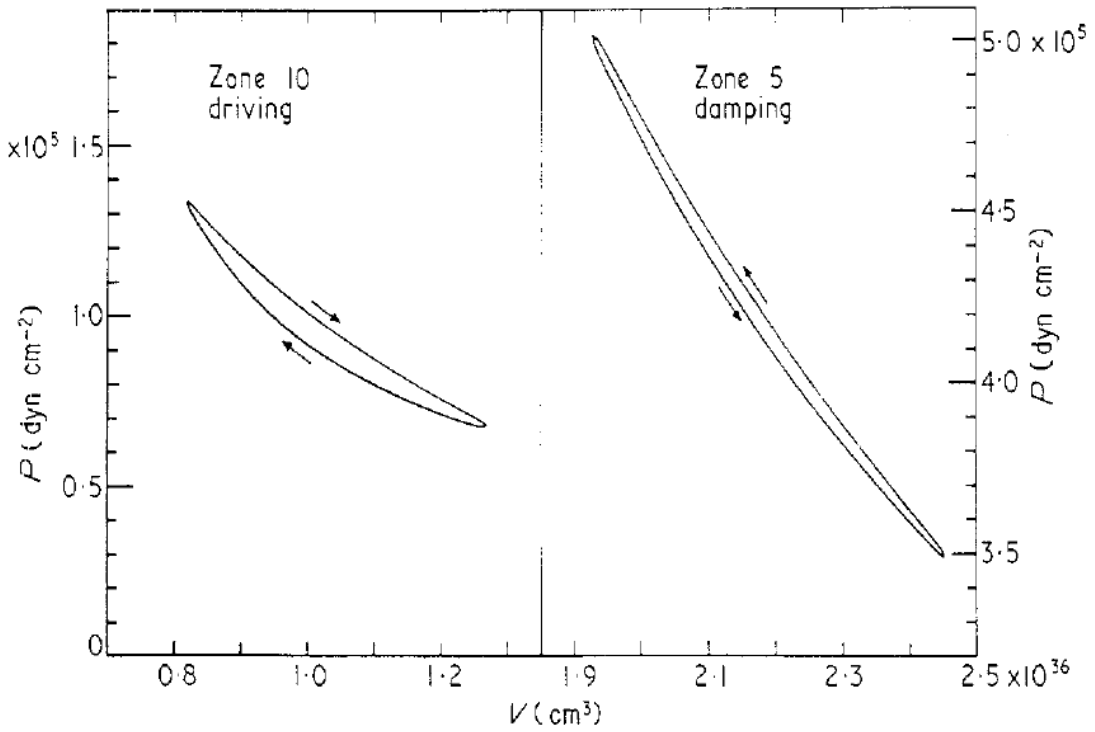


**Figure 15.** P–V plots for zones 10 and 5 for one of the classical cepheid envelope models investigated by Cox *et al* (1966) at limiting amplitude. The directions of the arrows show that driving is present in zone 10 (coinciding approximately with the region of 50% $He^+$ ionization, see text), while damping is present in zone 5 (below the $He^+$ ionization region). In the figure $V$ denotes the total volume of the zone (from King and Cox 1968).

Cox 1974

$$W = -\int \mathrm{d}^3x\, \nabla_{\mathrm{ad}} \oint \mathrm{d}t\, \mathrm{Re}\left[\left(\frac{\delta P}{P}\right)^* \delta\, \mathrm{div}\, \mathbf{F}_{\mathrm{R}}\right]$$

$$\nabla_{\mathrm{ad}} = (\mathrm{d}\ln T/\mathrm{d}\ln P)_{\mathrm{ad}}$$

$$\delta\, \mathrm{div}\, \mathbf{F}_{\mathrm{R}} = \frac{1}{4\pi r^2}\frac{d\,\delta L_r}{dr}$$

$$\frac{\delta L_r}{L_r} = \frac{\mathrm{d}r}{\mathrm{d}\ln T}\frac{\mathrm{d}}{\mathrm{d}r}\left(\frac{\delta T}{T}\right) - \frac{\delta\kappa}{\kappa} + 4\left(\frac{\delta T}{T} + \frac{\delta r}{r}\right)$$

$$\frac{1}{\kappa}\cdot\int \frac{dB_\nu}{dT}d\nu = \int \frac{1}{\kappa_\nu}\frac{dB_\nu}{dT}d\nu$$

$$\kappa_T + \kappa_\rho/(\Gamma_3 - 1)$$

$$\Gamma_3 - 1 = (\mathrm{d}\ln T/\mathrm{d}\ln\rho)_{\mathrm{ad}}$$

$$\kappa_T = (\partial\ln\kappa/\partial\ln T)_\rho$$

$$\kappa_\rho = (\partial\ln\kappa/\partial\ln\rho)_T$$

$$\tau_{\mathrm{th}}(r) = \int_r^R Tc_P\,\mathrm{d}M/L$$

**Pamyatnykh 1999 (due Dziembowski 1994)**

# Kappa-mechanism

## On excitation of pulsations

**$\varkappa$ - mechanism** :

$$\varkappa \sim \varkappa_0 \rho^n T^{-s}, \quad \begin{matrix} n \sim 1 \\ s \sim 3.5 \end{matrix}$$

($\varkappa$ - opacity coefficient)

(1) $$\frac{\delta T}{T} \sim (\gamma - 1) \frac{\delta \rho}{\rho}$$

In H- and He-ionization zones $\gamma \downarrow$ from $\sim 5/3$ to $\sim 1.1 - 1.2$

$\Rightarrow$ increasing effect of density variations on opacity variations during pulsations

$\Rightarrow \varkappa \uparrow$ at compression $\Rightarrow$ energy flux is blocked $\Rightarrow$ driving

Moreover, $n, s \neq$ const, their behaviour may also be in favour of driving ($s < 0$ in H-ioniz. zone)

(2) $$\text{Flux} \sim \frac{T^4}{\varkappa}$$

(due to ionization)

Direct influence of decreased temperature variations - **$\gamma$ - mechanism.** (see (1) and (2)).

Usually: „$\varkappa$-mechanism" = ($\varkappa$-mechanism) + ($\gamma$-mechanism).

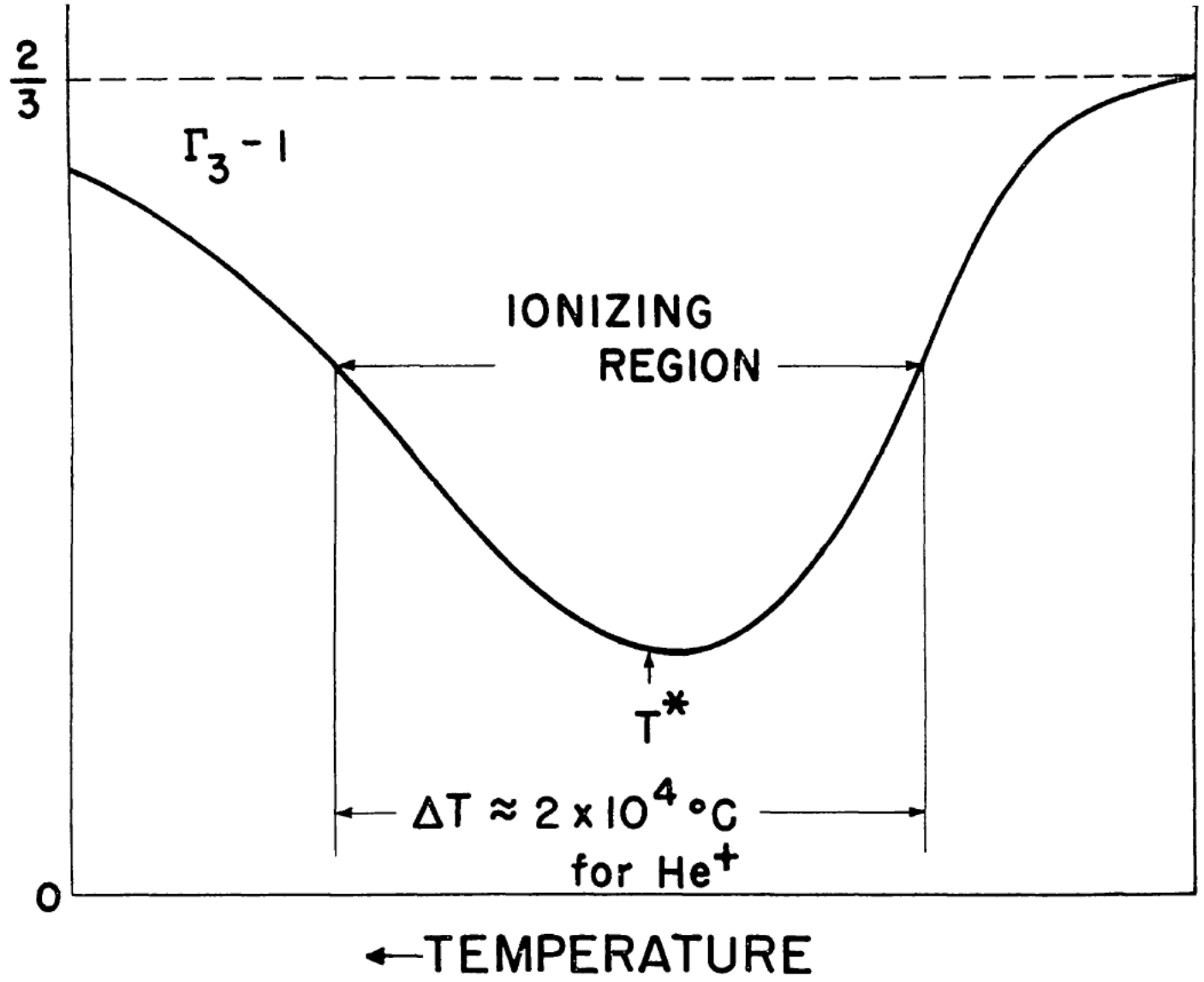


FIG. 4. $\Gamma_3 - 1$ vs. temperature (schematic) in the region of $He^+$ ionization in the equilibrium model of a stellar envelope.

Cox 1967

# Opacity mechanism

**Work integral** – net energy gained by an oscillation mode during one cycle:

$$W = -\int d^3x \cdot \nabla_{ad} \oint dt \, \frac{\delta P}{P} \, \delta \mathrm{div}\, \vec{F}$$

$$\delta \mathrm{div}\, \vec{F} = \frac{1}{4\pi r^2} \frac{d\, \delta L_r}{dr}$$

$$\frac{\delta L_r}{L} = \frac{dr}{d\ln T} \frac{d}{dr} \frac{\delta T}{T} - \frac{\delta \varkappa}{\varkappa} + 4\left(\frac{\delta T}{T} + \frac{\delta r}{r}\right)$$

- $\frac{d}{dr}\left(\varkappa_T + \frac{\varkappa_\rho}{\Gamma_3 - 1}\right) > 0$ for driving effect

**Two additional conditions** to excite an oscillation:

- In the driving zone, eigenfunction $\delta P/P$ must be large and must vary only slowly with $r$.
- In the driving zone, the thermal timescale

$$\tau_{th}(T) = \frac{1}{L} \int_{\text{surface}}^{M(T)} T c_p \, dM$$

must be $\gtrsim$ oscillation period.
Otherwise, the potentially driving region remains in thermal equilibrium during pulsation.

$$\tau_{\mathrm{th}}(r) = \int_{r}^{R} T c_P \, \mathrm{d}M / L$$

**Scala cieplna w obszarze wzbudzania**
**danego modu powinna być porównywalna z okresem oscylacji**

$T_{eff} > T_{eff,\ crit}$

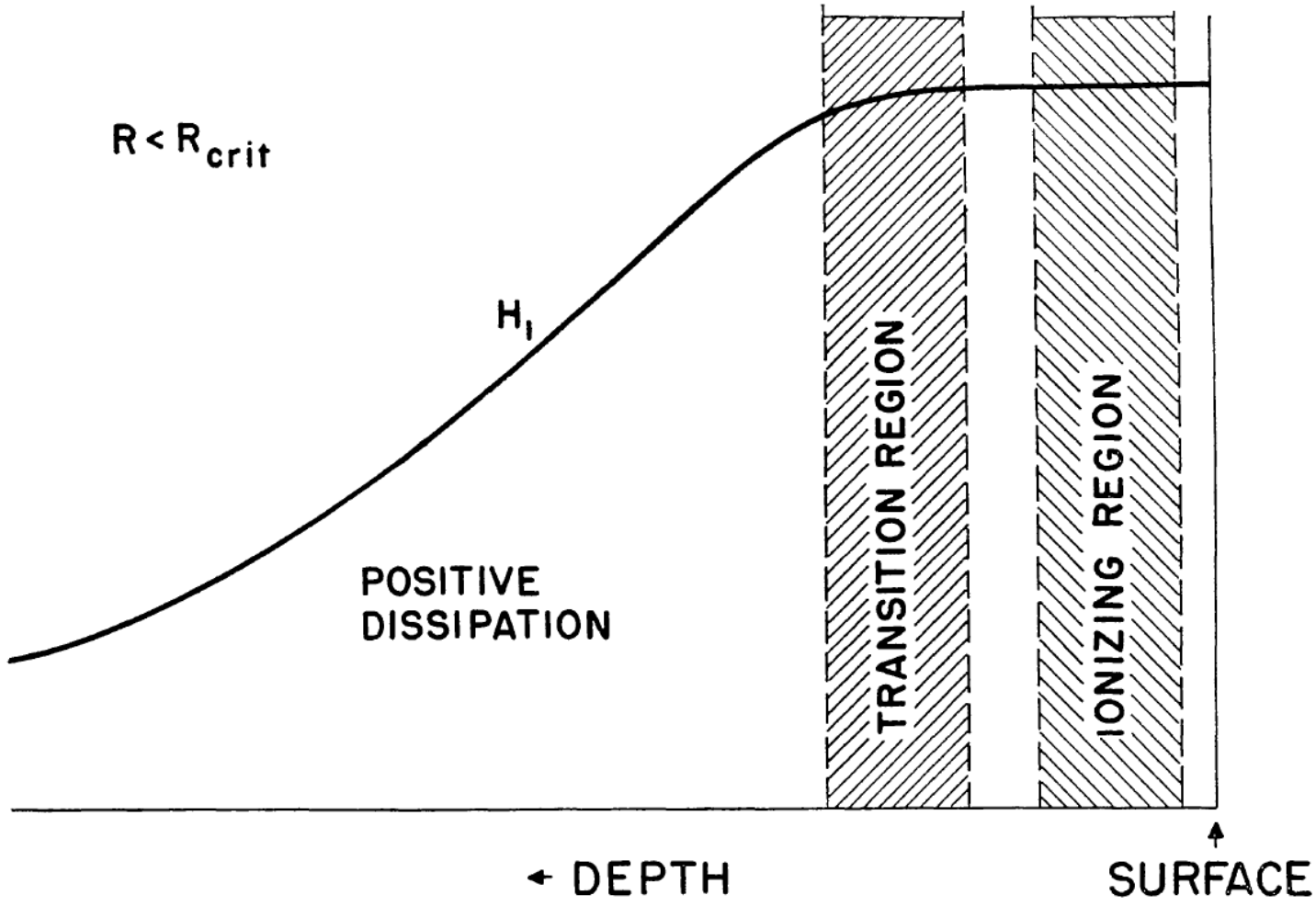


FIG. 5. $H_1$ vs. depth below the stellar surface (schematic) for $R < R_{crit}$ (see text for explanation of symbols).

$H_1 = Re(\delta L/L)$

Cox 1967

$T_{eff} < T_{eff,\,crit}$

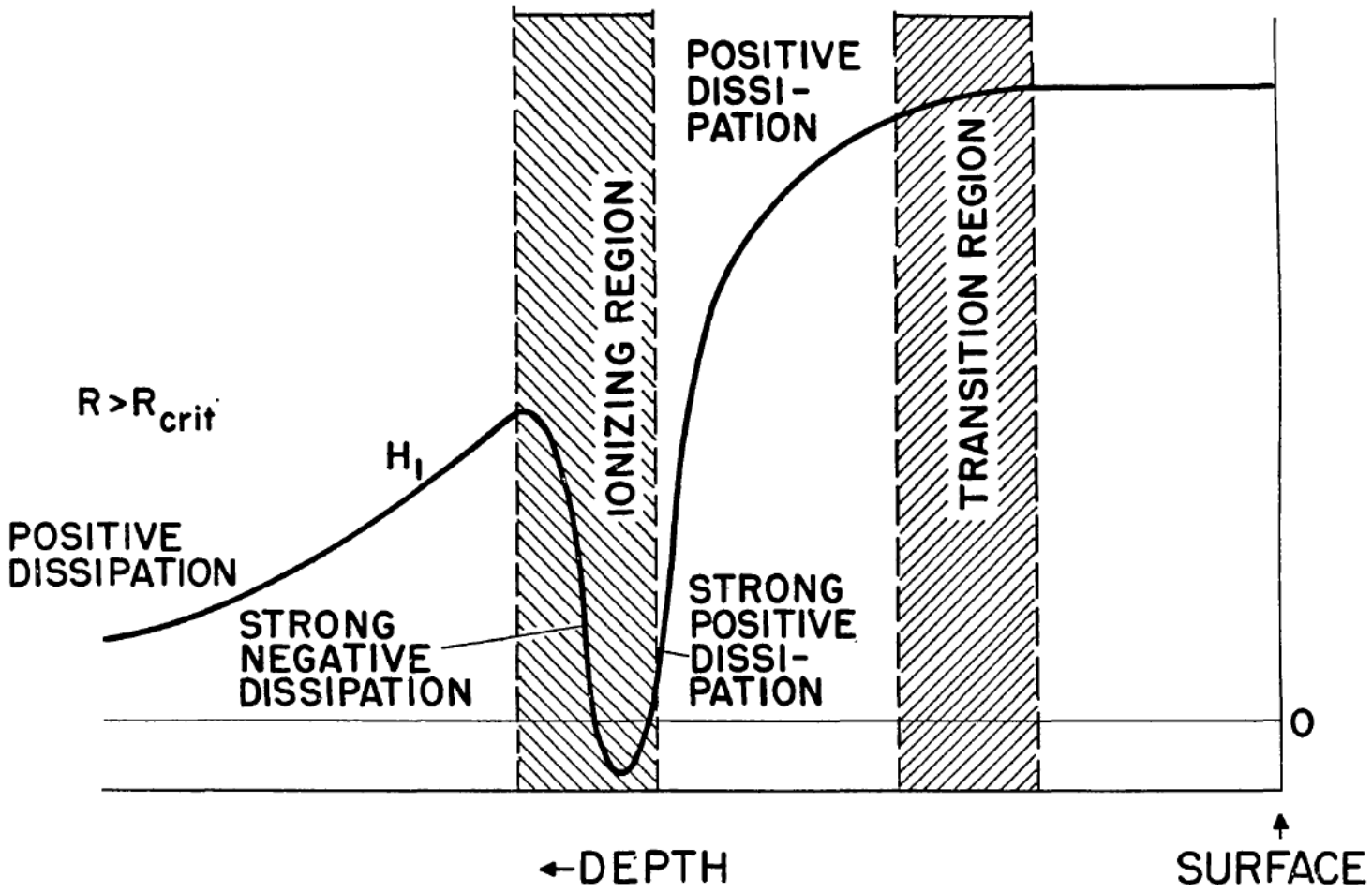


FIG. 6. $H_1$ vs. depth below the stellar surface (schematic) for $R > R_{crit}$ (see text for explanation of symbols).

Cox 1967

$T_{eff} = T_{eff,\,crit}$

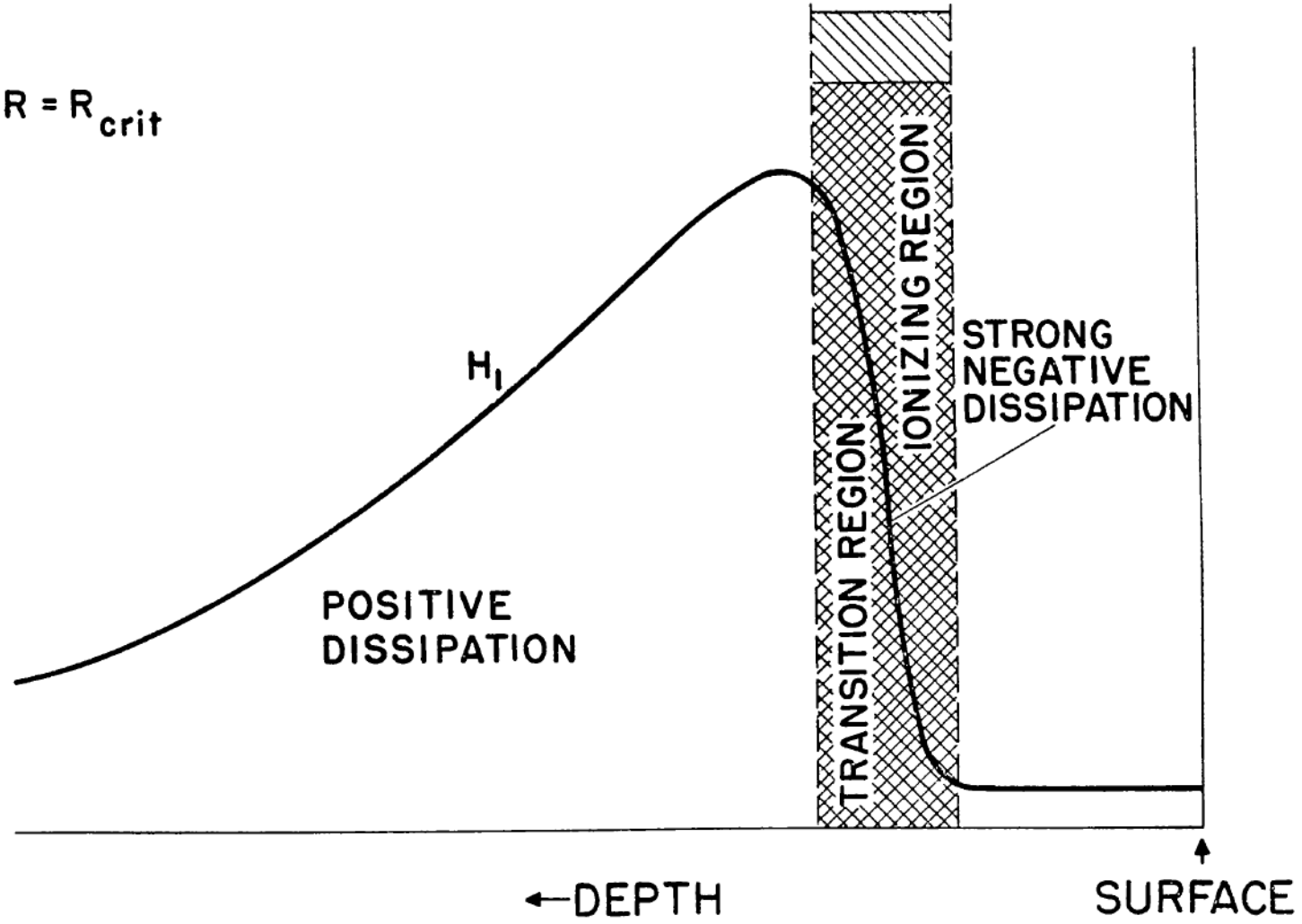


FIG. 7. $H_1$ vs. depth below the stellar surface (schematic) for $R = R_{crit}$ (see text for explanation of symbols).

Cox 1967

# Wzbudzanie pulsacji na Ciągu Głównym: Z-maksimum

## Opacity inside a Beta Cephei star model (M=12 Msun, X=0.70, Z=0.02): OP (Seaton et al.) *versus* OPAL (Livermore) *versus* LAOL (Los Alamos)

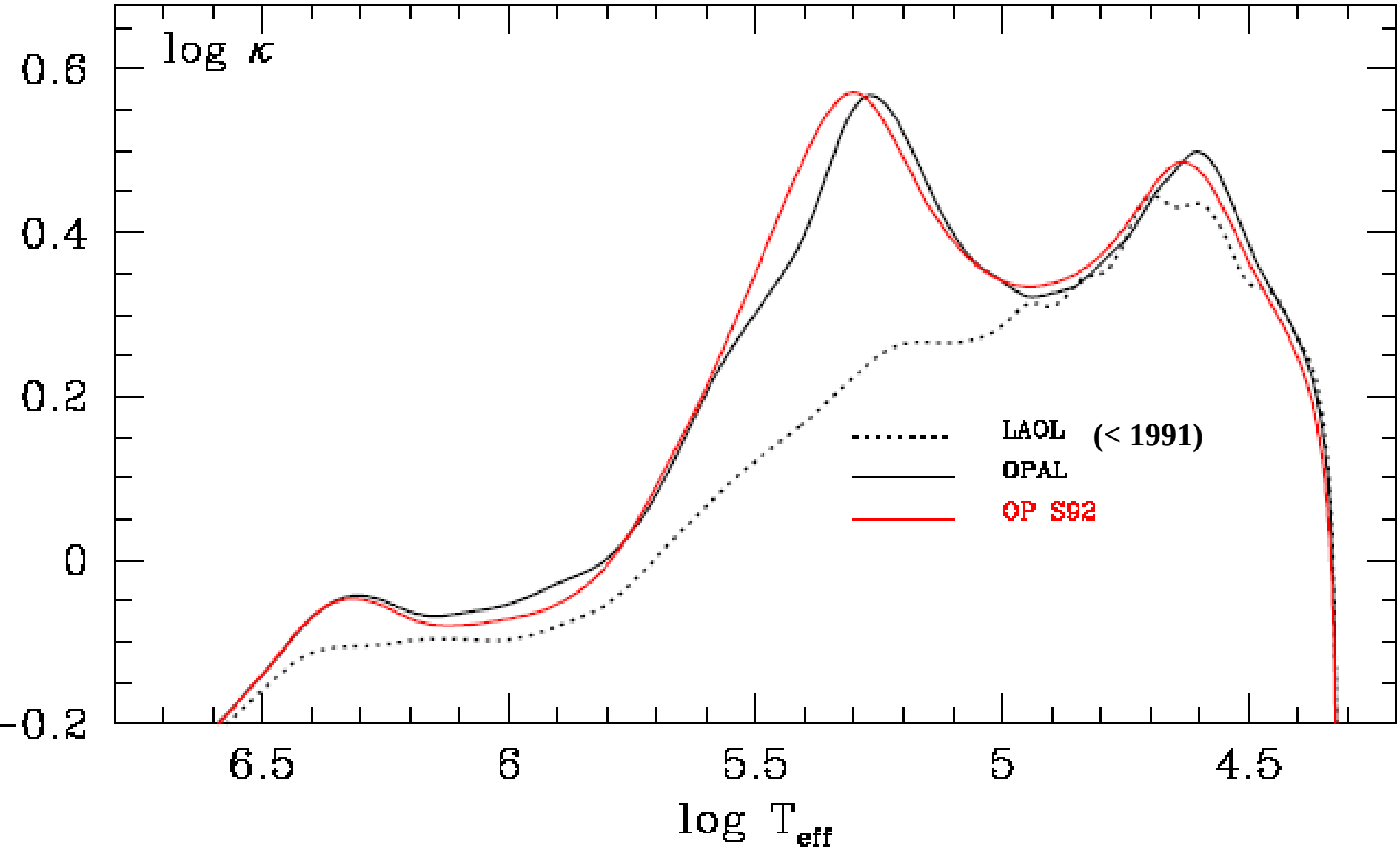

κ OPAL (1992) vs
κ OPAL (1991)

**Metal opacity bump is considerably increased and so is the driving effect**

**Work integral ( >0 for instability)**

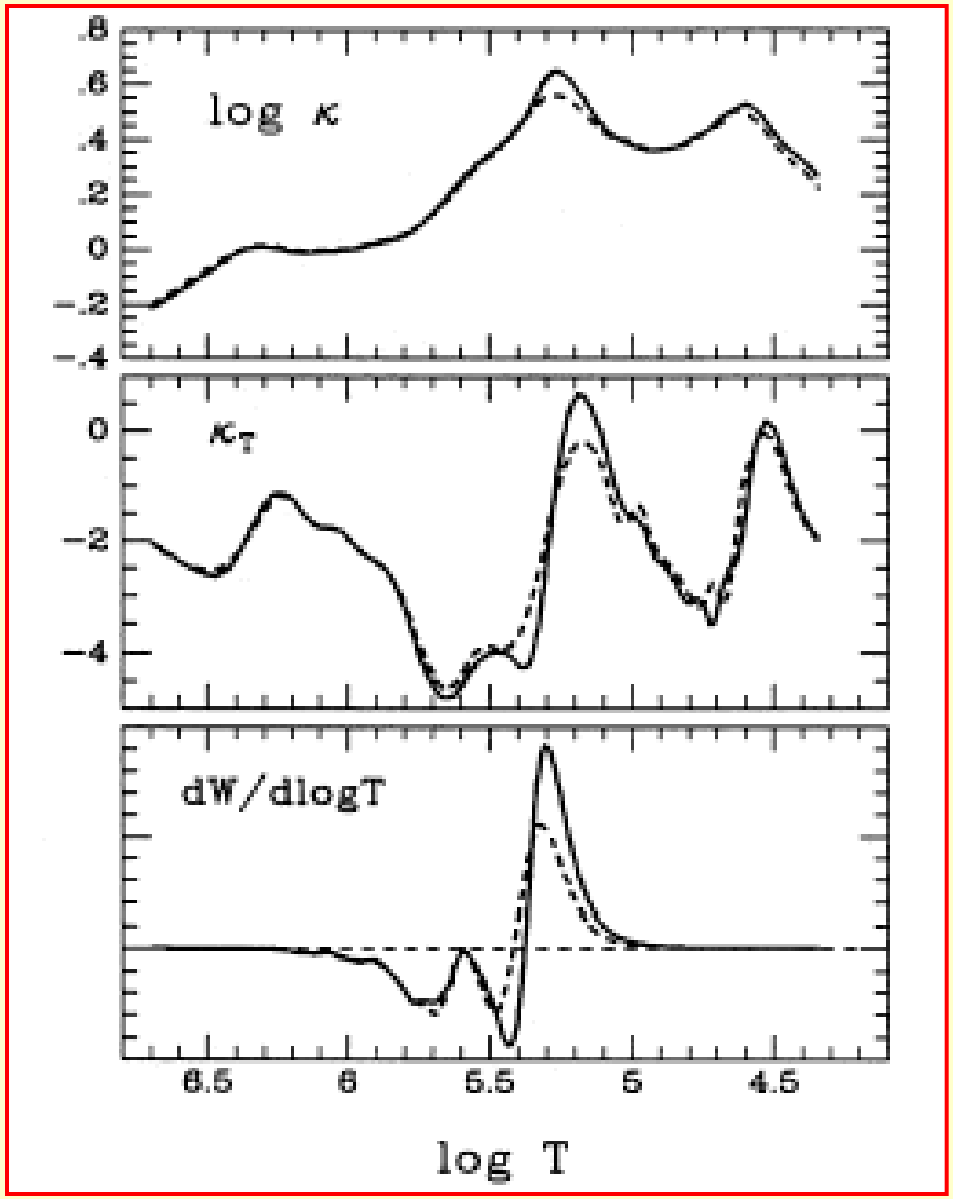


Dziembowski & Pamyatnykh, 1993, A&A, 262, 204

# Opacity behaviour at astrophysical conditions [κ OPAL 1996 ]

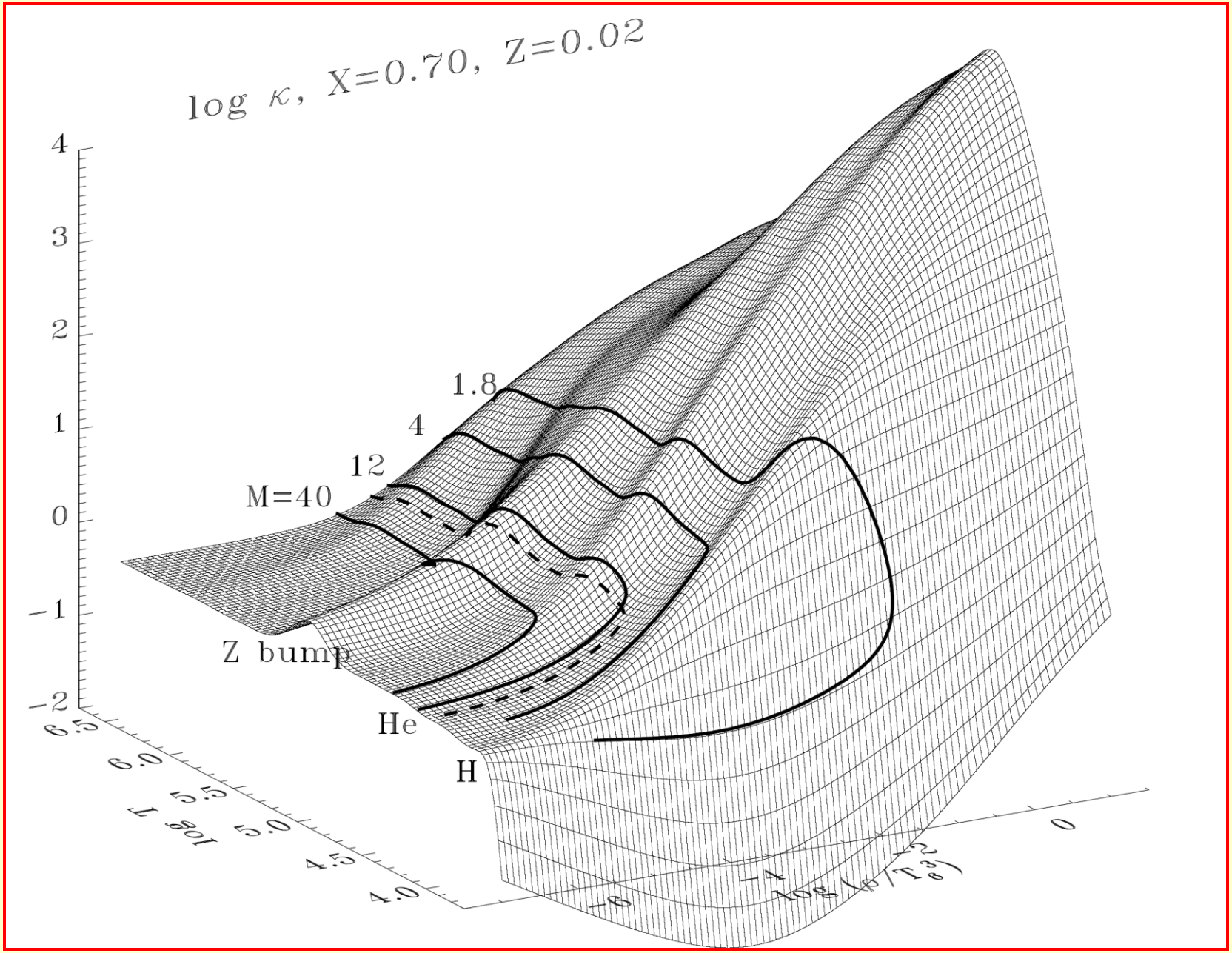


Pamyatnykh, 1999, Acta Astronomica, 49, 119

# Oscylacje βCep vs SPB vs δSct

Bierzemy trzy reprezentatywne modele:

**β Cep** -- M = 12 Msun , $T_{eff}$ = 23800 K

**SPB** -- M = 4 Msun , $T_{eff}$= 12450 K

**δ Sct** -- M = 1.8 Msun , $T_{eff}$=7280 K

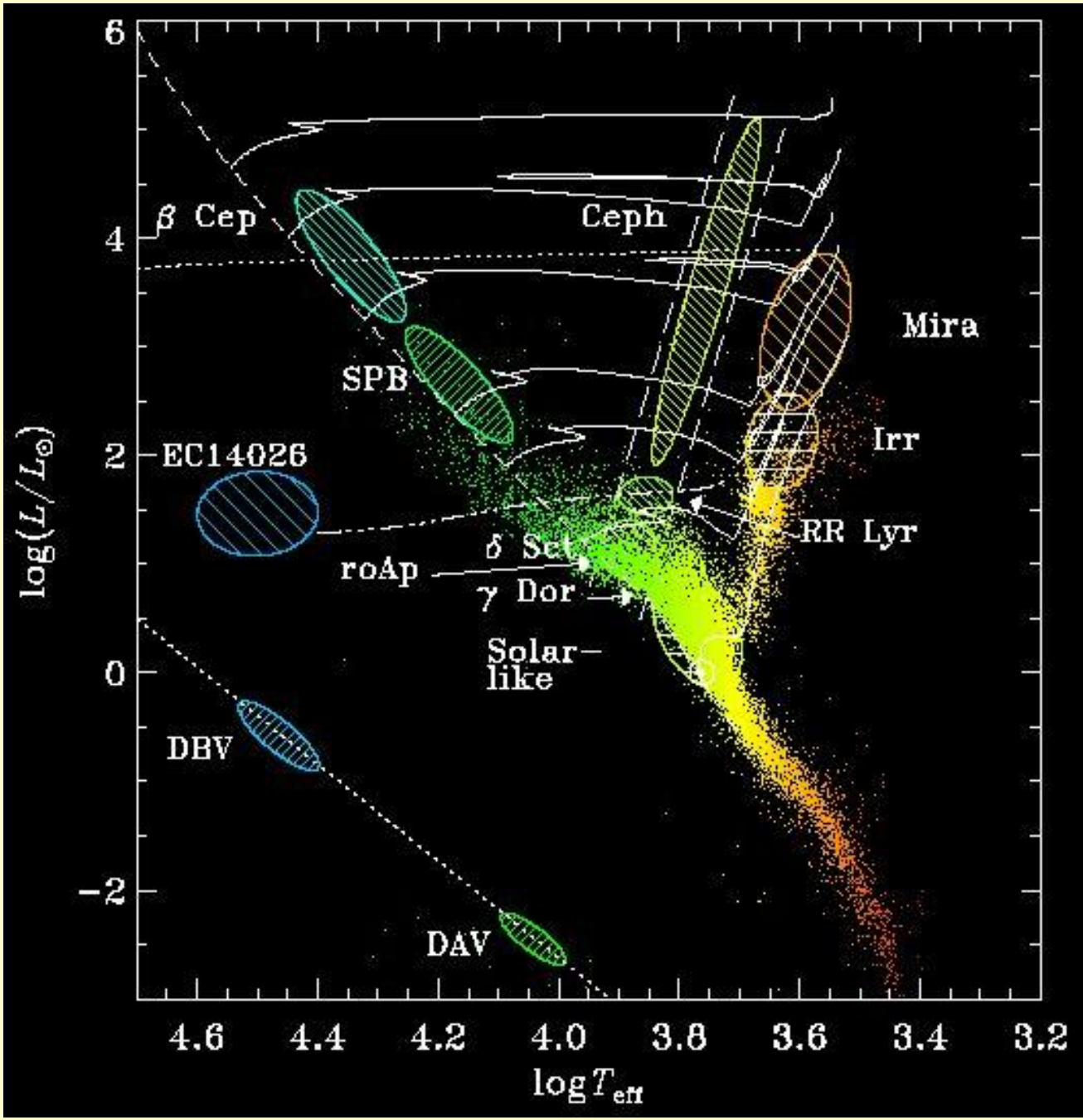


J. Christensen-Dalsgaard

# Opacity, thermal timescale and work integral for selested pulsation modes for three representative models of β Cephei, SPB and δ Scuti variables

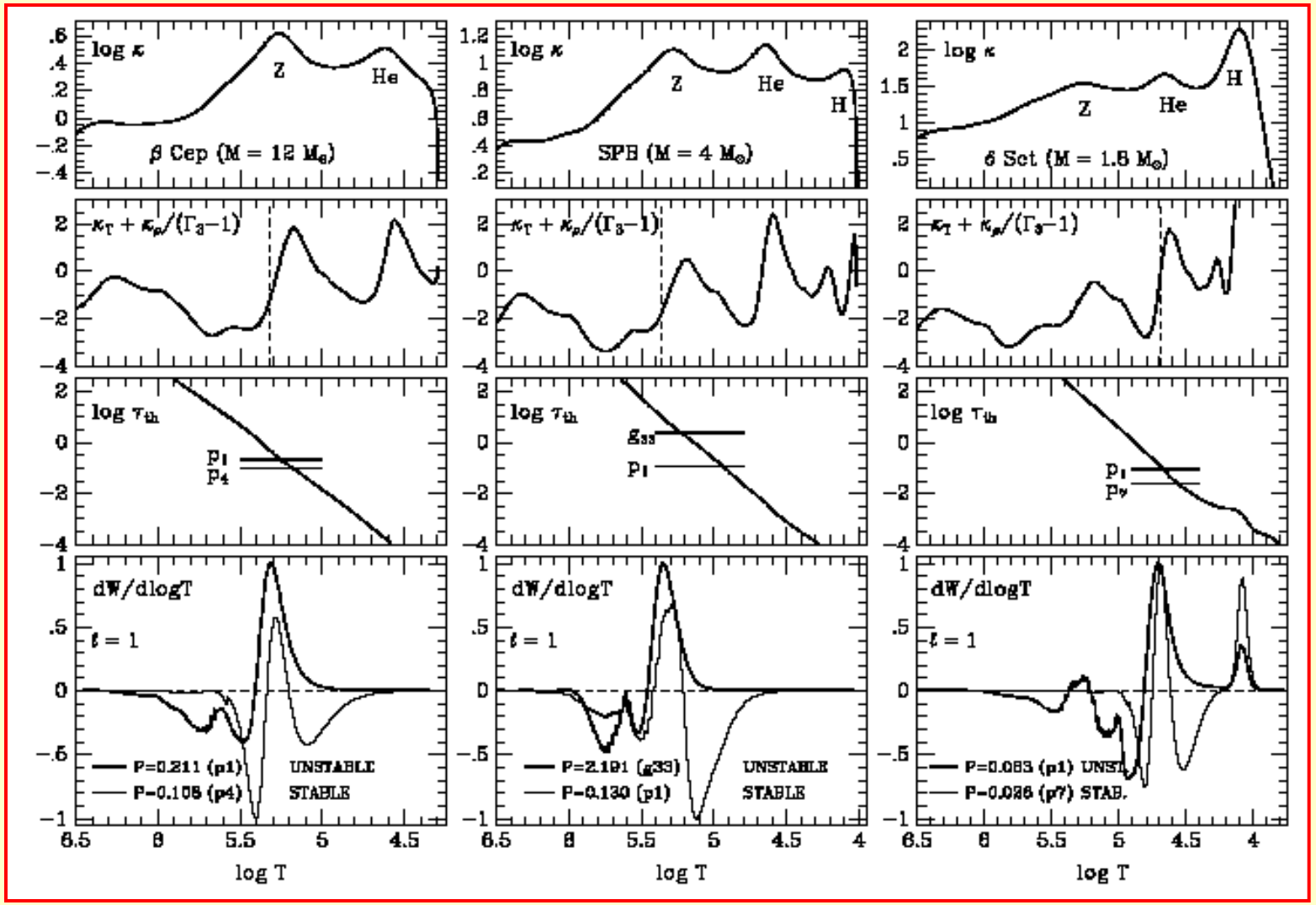


Pamyatnykh, 1999, Acta Astr., 49, 119

**Niestabilne mody $\ell=1$ dla poszczególnych modeli:**

**$\beta$ Cep** -- mody **$p_1$-$p_3$** o okresach od 0.211 do 0.153 dnia

**SPB** -- mody **$g_{53}$ - $g_{22}$** o okresach od 3.489 do 1.482 dnia

**$\delta$ Sct** -- mody **$g_2$ , $g_1$ oraz $p_1$-$p_6$** o okresach od 0.104 do 0.052 dnia

W modelu **β Cep** termiczna skala czasowa jest porównywalna z okresem pulsacji modów p o niskich owertonach.

Mody akustyczne o wysokich rzędach, n, są stabilne, ponieważ mają bardzo krótkie okresy i zaczyna działać tłumienie nad obszarem „bumpu” metalowego.

Mody grawitacyjne o dłuższych okresach są stabilne, z powodu krótkiej termicznej skali czasowej oraz silniejszego tłumienia poniżej obszaru „bumpu” metalowego.

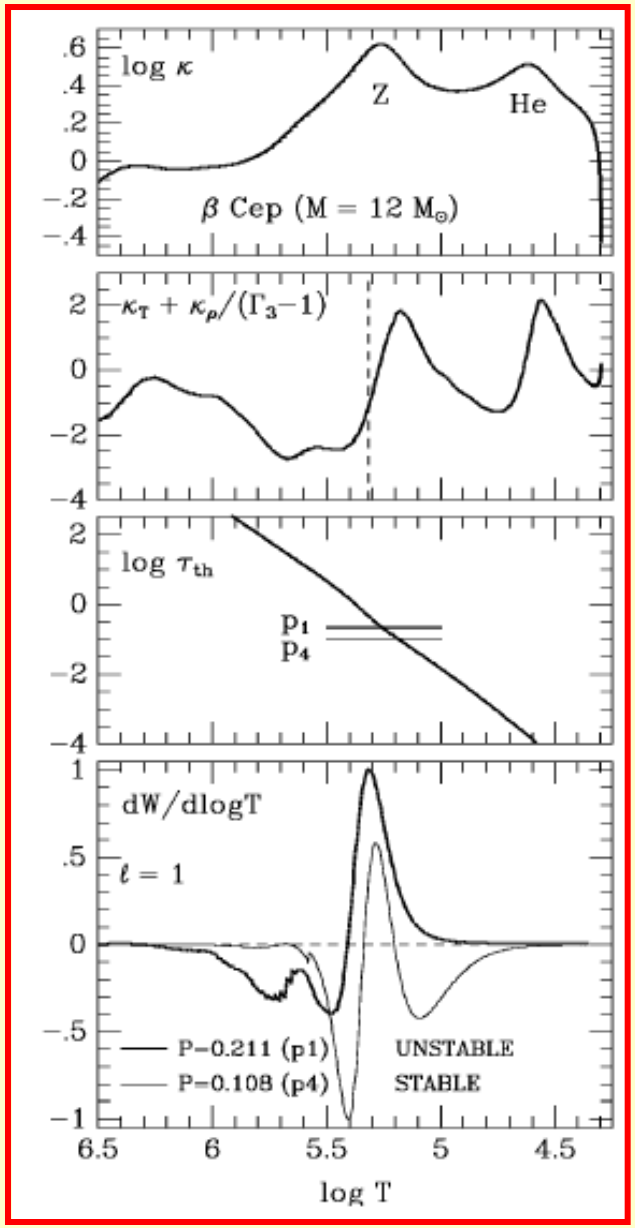


(JDD Wrocław)

W modelu **SPB**, termiczna skala czasowa w obszarze „bumpu” metalowego jest 20x dłuższa, gdyż jest on położony dużo głębiej. $\tau_{th}$ jest porównywalna z modami g o wysokich owertonach.

Mody p i g niskich rzędów są stabilny, ponieważ dla tak krótkich okresów zaczyna działać warstwa tłumiąca znajdująca się pomiędzy „bumpem” metalowym i helowym.

Widmo modów grawitacyjnych jest bardzo gęste.

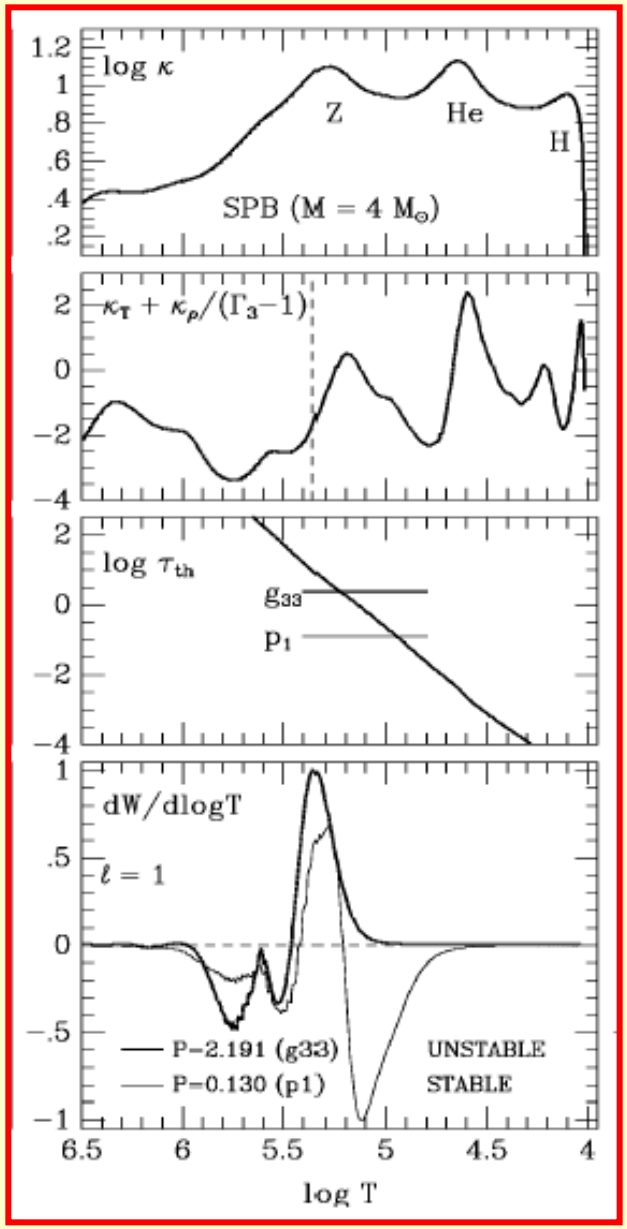


(JDD Wrocław)

W modelu δ Sct wzbudzane są mody p i g niskich rzędów radialnych , n.

Mody p wyższych rzędów są tłumione przez warstwę położoną pomiędzy „bumpem” helowym i wodorowym.

Mody g wyższych rzędów są stabilne z powodu warunku na $\tau_{th}$.

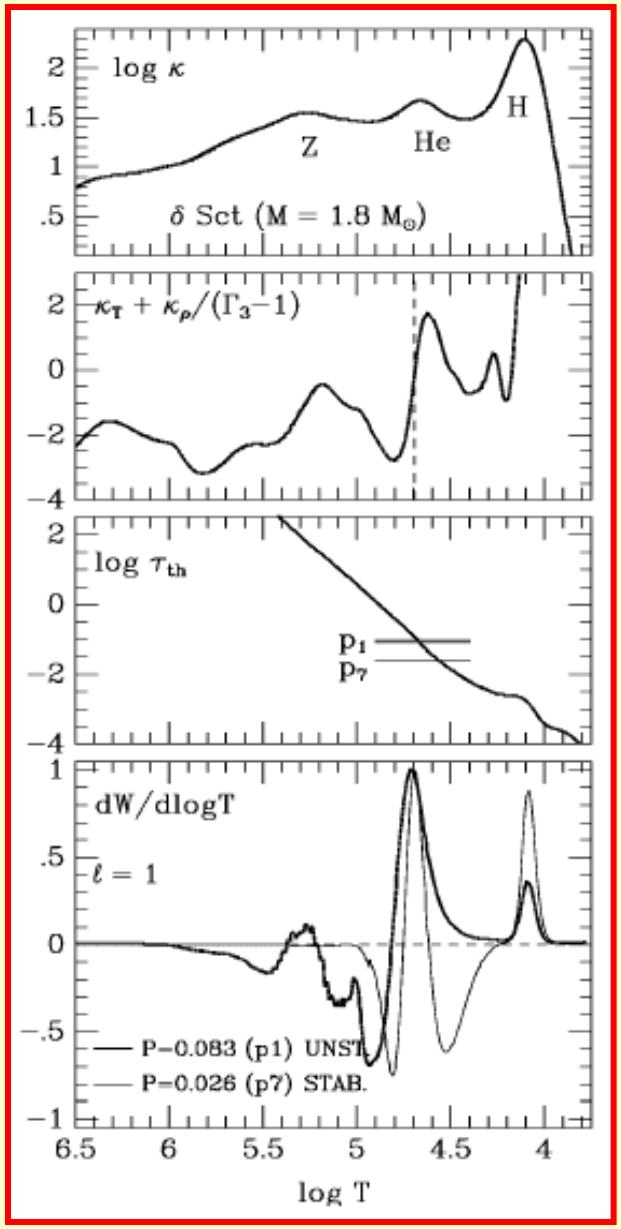


(JDD Wrocław)

# Tablice nieprzezroczystości OPAL i OP

Źródła różnic miedzy tablicami:

- Inne podejścia do liczenia nieprzezroczystości
  - Równanie stanu
- Obfitości poszczególnych pierwiastków (2 - 5%)

„Bump” metalowy dla danych OP jest położony głębiej przy temperaturze ~15000-20000 K wyższej.

**Różnice między OPAL i OP dla modelu β Cep (M=12Msun , log$T_{eff}$= 4.24), dla fundamentalnego modu radialnego. Mod ten jest niestabilny tylko dla OPAL.**

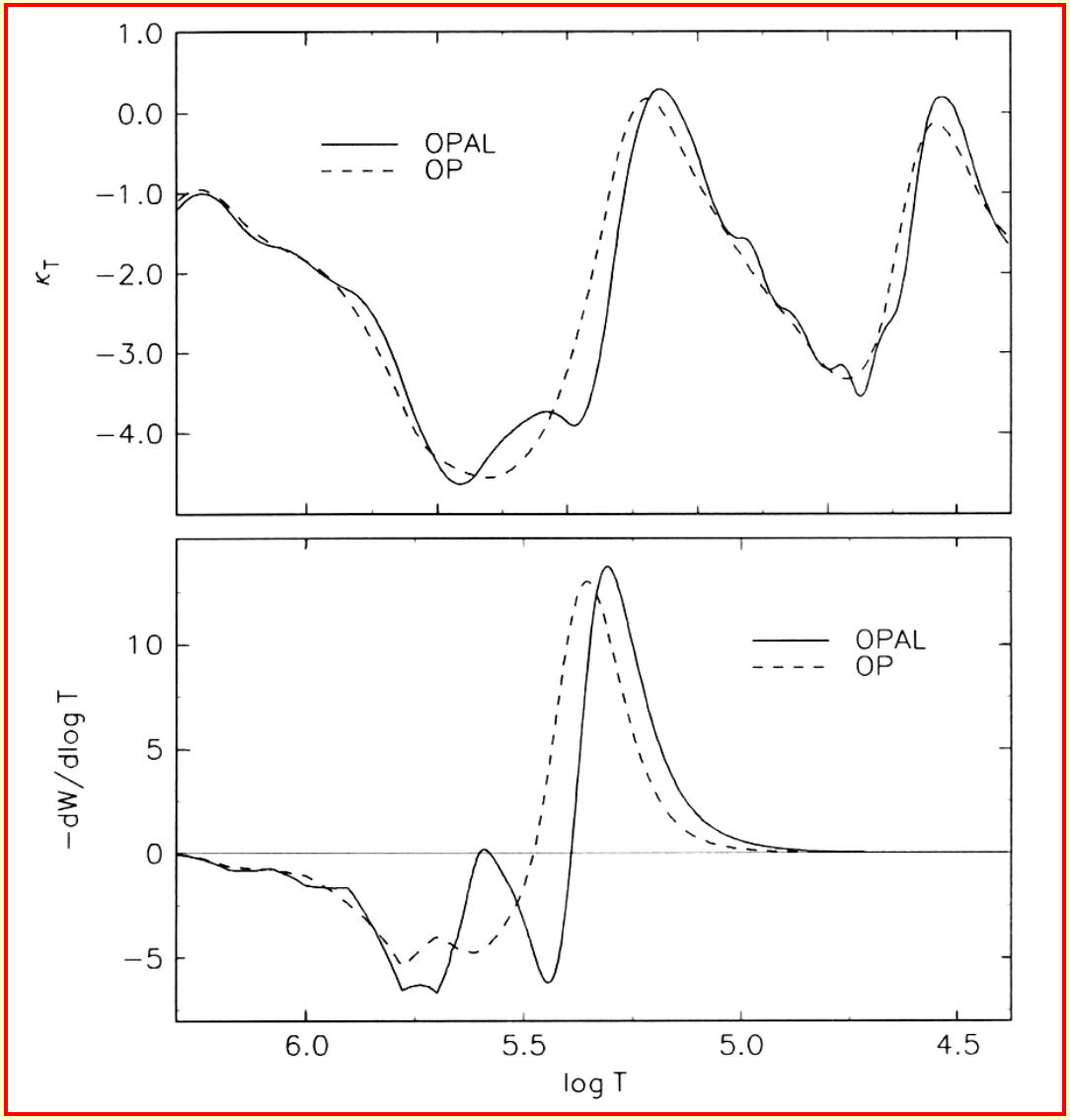


(JDD Wrocław)

**W.A. Dziembowski 1994**

Obszary niestabilności wyliczone z tablicami **OPAL**.

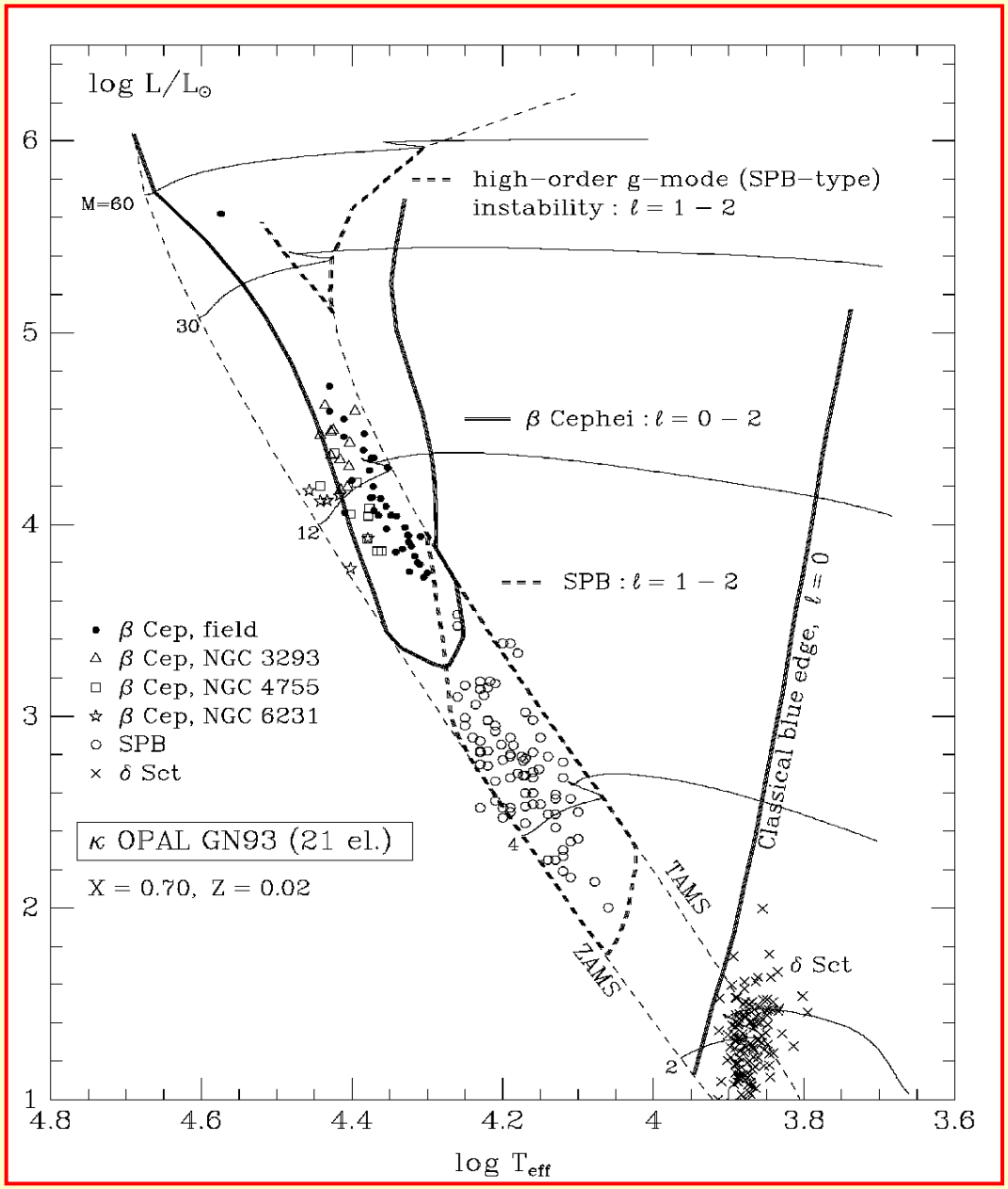


(JDD Wrocław)

**Pamyatnykh 1999, AcA 49, 119**

Obszary niestabilności wyliczone z tablicami **OP.**

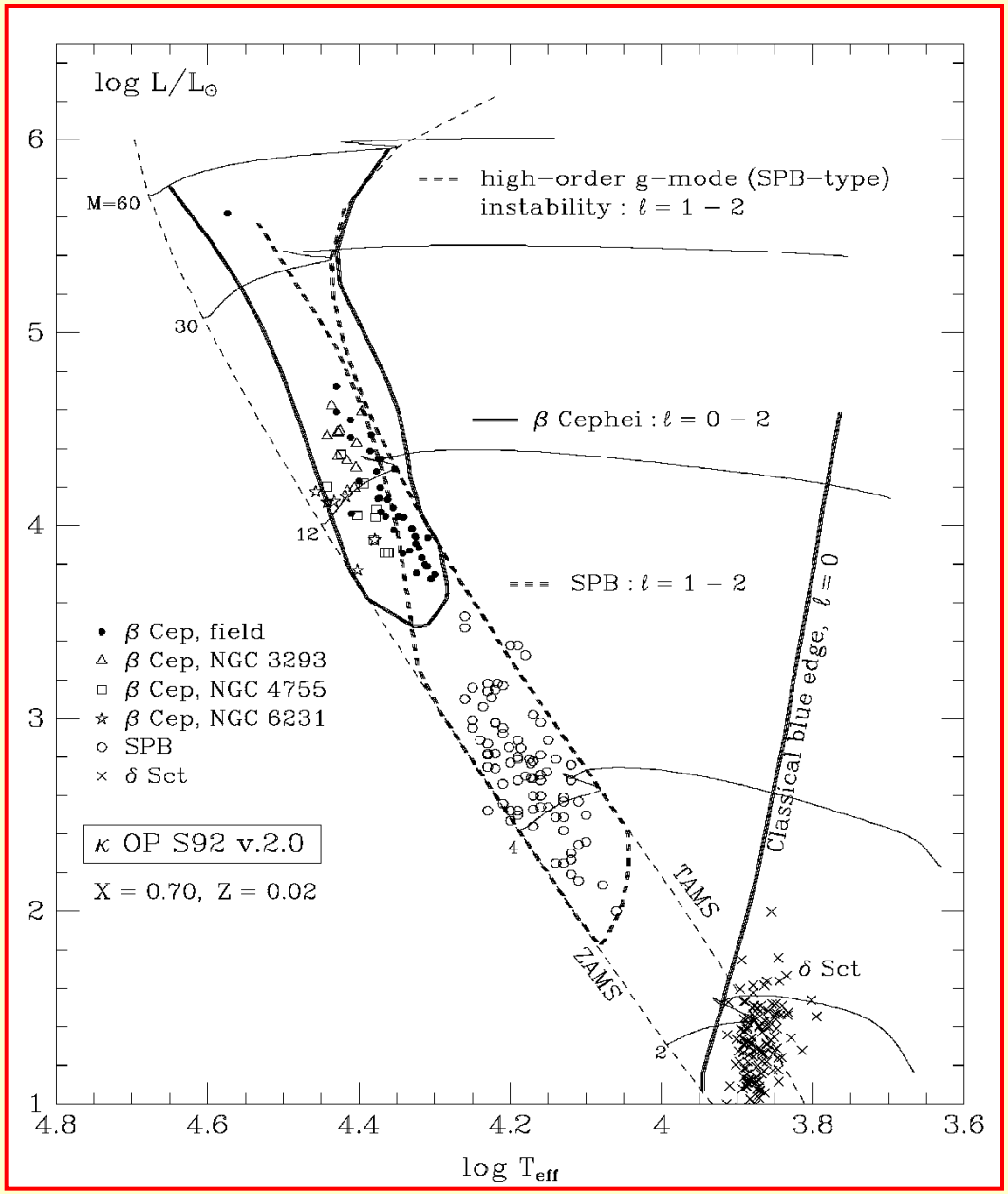


(JDD Wrocław)

**Pamyatnykh 1999, AcA 49, 119**

# Okresy modów niestabilnych w obszarze β Cep i SPB

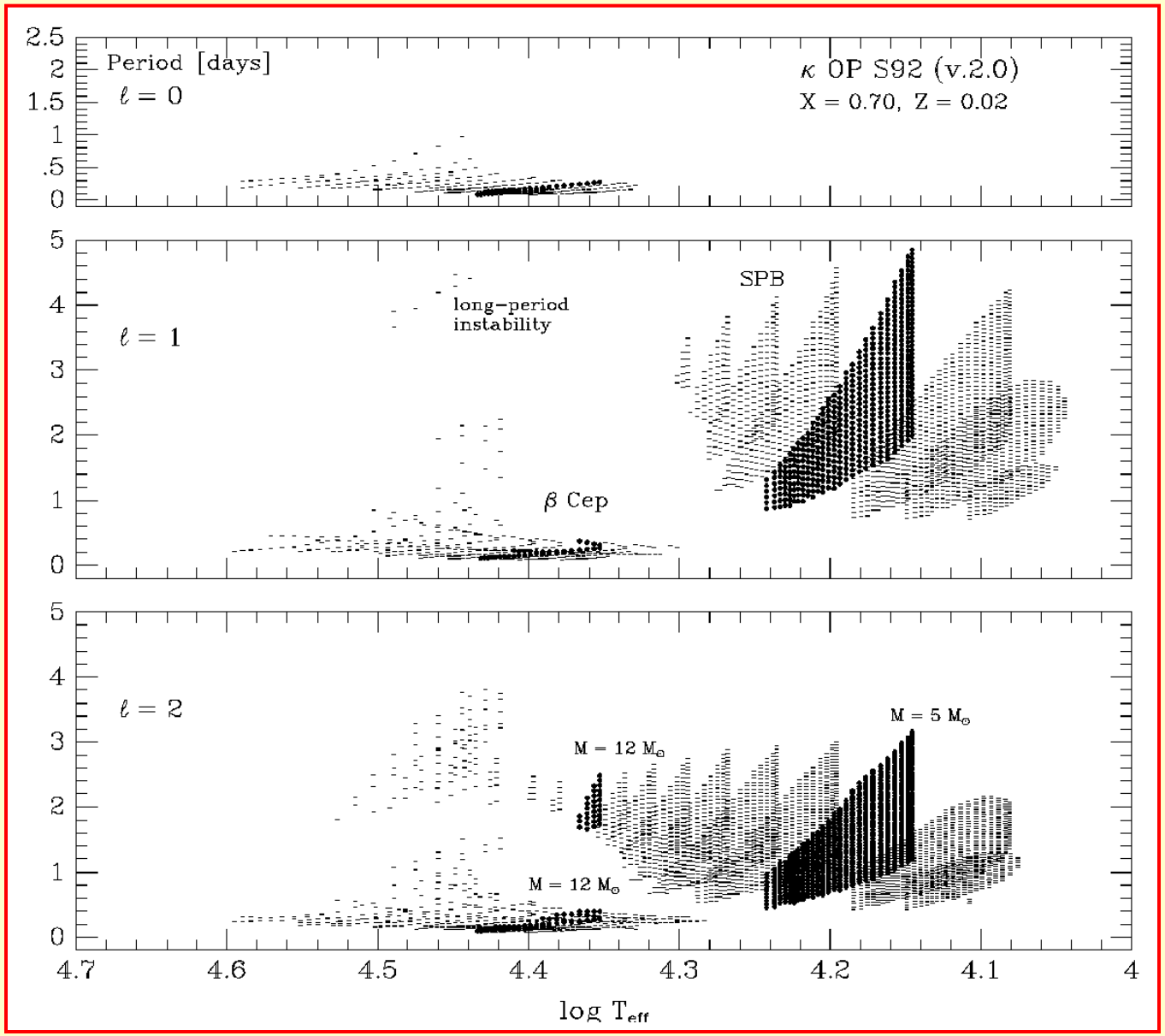


(JDD Wrocław)

Pamyatnykh 1999, AcA 49, 119

**Effect of changes in the heavy element abundances on evolution and stability of the upper MS stars:**

**κ OPAL,**
**Z = 0.01, 0.015, 0.02**

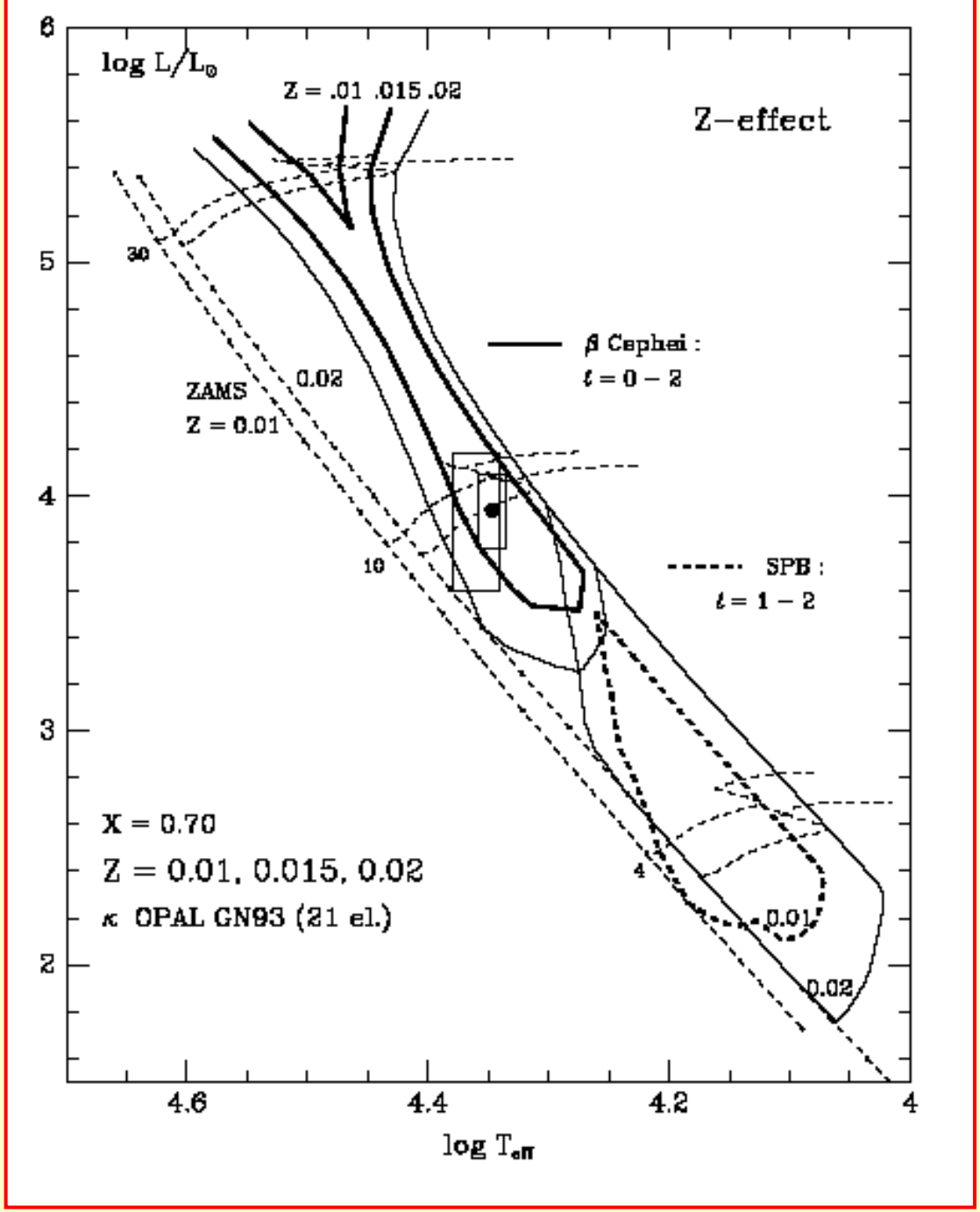


Pamyatnykh, 1999, Acta Astr., 49, 119

Obfitość metali, Z, ma największy wpływ
na obszary niestabilności gwiazd typu B.

Efekt ten jest dwojakiego rodzaju:

- zmiana struktury gwiazdy i jej ewolucji
- zmiany efektywności mechanizmu napędzania

(JDD Wrocław)

# The END